Quarterly Report
on
Long Endurance Underwater Power System

October 1988 - December 1988

Contract No. N00014-87-C-0335

Aquanautics Corporation
980 Atlantic Avenue, #101
Alameda, CA 94501
January 28, 1989

TABLE OF CONTENTS

1. Executive Summary

The development and design of deep sea power sources for long endurances (>1 year) and moderate power (>1 KW) are quite unique. The best primary battery (Li-Thionyl Chloride) would involve huge space (14,000 liters) and weight (20,000 kg.) and the cost of such a system would be prohibitive. Fuel cells with stored gases will need a pressure vessel and also quite a large volume and weight. Aquanautics' unique technology is well-poised to deliver such a system of a very demanding design. Aquanautics is engaged in developing such a power source. The design would involve a completely open system eliminating the need for a pressure vessel. Aquanautics will capture oxygen from the seawater to be delivered to a fuel cell. The hydrogen generated in this design is envisioned to be from a reaction between Aluminum and seawater. Such a completely open system is already available from Alupower, Inc. This provides for a much safer and more compact design than cryogenic hydrogen. Lithium or Magnesium can also be used. Both are expensive and Lithium is known to be potentially hazardous.

To develop this technology, Aquanautics will need to retire certain technical issues and is aggressively working in order to do that. The following table provides these issues, their performance targets and progress made during the last quarter. The performance targets have been chosen so that our system is much better than any other competitions that may exist.

Key Technical Issues, Targets and Progress

	Performance Targets		Status
	Demo	Real	12/88
1. Direct Feed Fuel Cell, W-min/l O_2	100	160	Being developed
Inclusive of cell, if required. volume, l/KW	-	500	
2. Carrier			
Longevity, yrs.	0.09	2	0.09
3. Gill Membrane			
a) Depth, meters	600	6000	Not tested yet
b) Durability, years	0.09	2	Not tested yet
c) Volume l/l of O_2	-	500	400*

*For microporous membranes, solid membrane on test.

Since the last report (Final Report on the Artificial Gill Program - October 28, 1988), there has been major improvement of the technological issue of carrier longevity. The previous carrier that was used had an operational life of 3 days. At present, Aquanautics has discovered a carrier called 23SuzyP which has stable electrochemical performance for over a month. We have also received a report from Alupower which shows that H_2 (result of corrosion of Aluminum) at these depths would still be available mainly as gas. This retires a technical issue of having to develop a fuel cell with dissolved hydrogen.

Cell scale-up work has been completed. There is some cell-to-cell variation which needs to be investigated. There has been some progress on kinetics and carrier screening methodology. Preliminary cell modeling has also been completed. More refinement will be carried out later.

2. Engineering Progress

This section summarizes the activities of the engineering personnel during the last quarter (October 1988 - December 1988).

The following reports are attached:

1) Cell Modeling Report
2) Cell Scale-up

The major findings in the activities of gill, Ceramatec, Allied-Signal, Cell Symposium Trip and Alupower (DARPA) are also covered in this report.

1. Cell Modeling:

In cell modeling, the cell voltage at a given current density were accounted for. The experimental results were within the range predicted by the model.

The experimental cell performance at higher current densities was however worse than that can be expected by the model. Limiting mass transfer rate of oxygenated species in the anode and that of the oxidized species at cathode at the graphite felt electrodes are much higher than the corresponding current densities at which the experiment shows a limiting behavior. This shows that the kinetic mechanism chosen does not apply in the higher current density region. From mass transfer rate calculations, fractional conversion would be higher than 0.5 for the experimental range of flow rates. In the next quarter, this model will be refined.

2. Gill:

Charles Benedict has studied the fouling mechanism and determined that fouling at depths below 1000 M or so will be minimal. A membrane testing rig has been constructed. A few solid membrane samples and cartridges from various sources have been obtained. A model was also built to determine the sensitivity of membrane permeability on overall oxygen transfer rate from seawater to carrier. This shows that with existing solid membranes, this should not make much difference. The membrane testing data will prove or disprove it.

In this quarter these membranes will be tested and a fouling test will be initiated. Charles Benedict will also write a report in this quarter regarding these.

3. Cell Scale-Up:

Efforts to make a multi-cell stack resulted in ambiguous data. The major side issues were passive flux of oxygen and unloader efficiency. The passive flux when N_2 is used as sparge gas was seen to be minimal. The unloader efficiency with no sparge gas was seen to be erratic. However, with sparging, the unloader efficiency was seen to be close to 100%. Unloader design with no sparge gas still seems to be a major problem.

The performance difference between monopolar and bipolar cell stacks could not be resolved. The performance difference between monopolar and bipolar stacks could be totally attributed to the cell to cell variation. In this quarter, we shall investigate the cause for this variation.

4. a. Ceramatec:

Ceramatec has a high temperature solid-oxide oxygen generation system. One of their applications which incorporates the Aquanautics system is heat engine. Here the Aquanautics system would compress oxygen 2-7 decades from 10^{-5} to 1 atmosphere, at room temperature. At high temperatures, solid-oxide systems would produce power from the pressure difference. The thermal efficiency of the system would be large compared to other alternatives. This particular application is quite unique for Aquanautics. There is no other efficient process for compression of oxygen at room temperature.

b. Allied-Signal (and Garret AiResearch):

Their MSOFC (Monolithic Solid Oxide Fuel Cell System) system was looked at as a possible hook-up to Aquanautics gill technology for the AUV. This seemed to be a logical step specially if MSOFC could utilize diesel as a fuel. Computer modeling was carried out and the results were sent to Al Ellinthorpe for his information.

c. Alupower:

A contract was granted to Alupower Inc. to look at the hydrogen generation by their Al-Watt system. The report is in and Alupower's results indicate that their system will generate about 25% of the total power and 11-100% of hydrogen could be in the dissolved form.

At a depth of 1000 M and $0^{o}C$, Alwatt would generate about 2500 litres (STP)/hour from 1 sq. m. cell area operating at 10 mA/cm^2. This is capable to generate 1 KW power. The hydrogen generated will produce 4 KW power in a fuel cell. A maximum charge of 200m Ah can be passed in a milliliter of seawater before Al-hydroxide clogs the Alwatt battery. A design point of 10 mAh/ml has been chosen. At this point, most of H_2 will be in gaseous form. The report is included in the Appendix.

2.A Voltage Loss Calculation for Aquanautics Cell

Summary:

The calculated voltage losses are approximately the same as those found in the experiments. It was determined first that we are in the kinetic controlled situation rather than mass

transfer. The voltage loss in kinetic case is calculated using exchange current density and transfer coefficient values obtained from our scientists. Also I included some other resistive losses.

I believe, though that the true rate limiting mechanism is more complicated than what I assumed. For instance, our reaction is mediated. The true mechanism is believed to be the electron transfer to a mediator at the anode and then chemical reaction of the oxidized mediator and the L-Co-O_2-Co-L compound (L stands for ligand). In the near future, we would like to incorporate a more refined and accurate model to describe the V-I relationship in our cell.

1. Introduction:

The following calculations are carried out to primarily determine the voltage losses in the Aquanautics cell. The method has been to determine:

1) Mass transfer limiting situation

2) Calculate the losses under kinetic controlled situations given that mass transfer is not limiting.

These calculations are to be considered approximate.

2. Mass Transfer

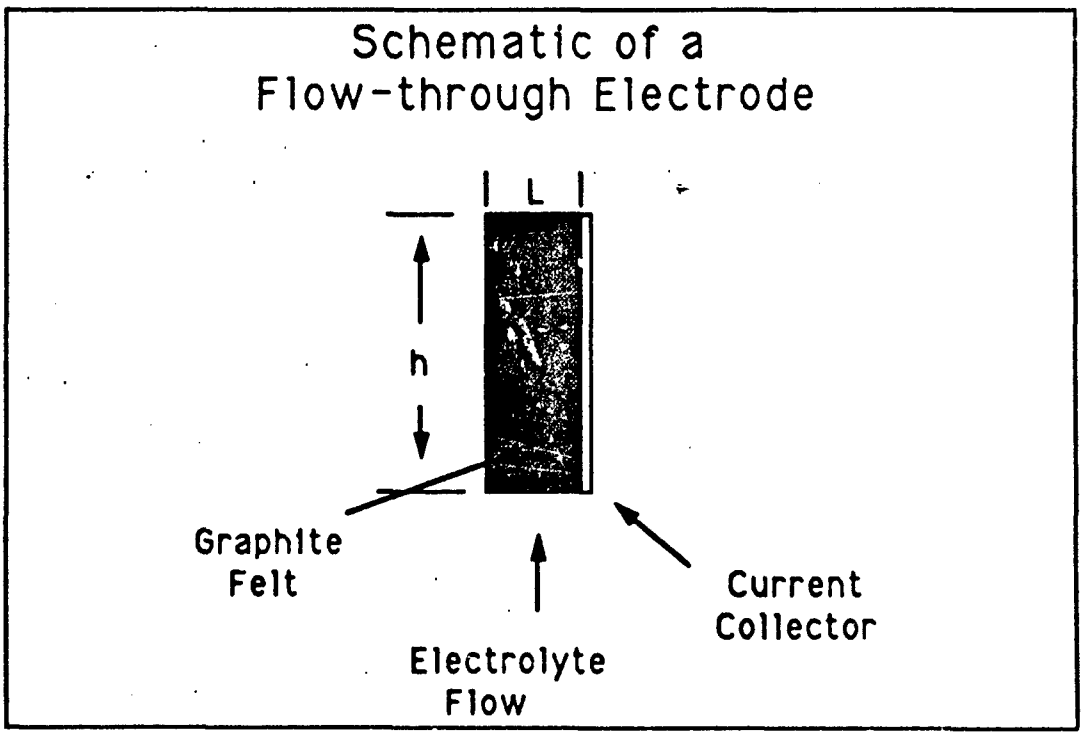

In our situation, the flow of our electrolyte is perpendicular to the current.

Principal anodic reaction:

$$(L - Co^{++})_2 - O_2 \text{ ---> } 2L - Co^{+++} + O_2 + 2e^- \quad (1)$$

Principal cathodic reaction:

$$L - Co^{3+} + e^- \text{ ---> } L - Co^{2+} \quad (2)$$

To determine whether the electrode is operating near mass transfer controlled region, one needs to calculate the limiting current.

Km, mass transfer co-eff, can be calculated from Wilson & Geankoplis equation (Ref. 1, p. 366, equation 11) as:

$$Km = 1.09 \frac{Do}{\varepsilon Dp} \left(\frac{\vartheta Dp}{Do}\right)^{1/3} \quad (3)$$

where Do is diffusivity co-eff. (2.to 4.10^{-10} m^2/s)

ε is porosity (0.94)

Dp is particle diameter (1.10^{-5}m)

ϑ is velocity (2.10^{-3} - 18.10^{-3} m/s)

This is valid only when $\vartheta/a\upsilon$ (υ is kinematic viscosity, a is specific surface area) is between 5.10^{-4} and 15. In our case, since ϑ = 2.10^{-3} to 18.10^{-3} m/s, a = $1.32\ 10^{+4}$ m^{-1}, υ = 1.10^{-6} m^2/s,

$$\frac{\vartheta}{a\upsilon} = 0.15 \text{ to } 1.35$$

So this equation holds good.

$$\therefore Km = \frac{1.09}{\varepsilon} \left(\frac{Do}{Dp}\right)^{2/3} \vartheta^{1/3} \quad (4)$$

$$= 0.018\ \vartheta^{1/3} \text{ in MKs units in our case}$$

$$= 1.10^{-4} - 2.10^{-4} \text{ m/s}^{\text{Footnote 1}}$$

Footnote 1 Kinoshita et al (3) have investigated mass transfer in graphite felt and found the following relationship for a 0.25 cm thick electrode.

$$Km = 1.29 \frac{Do}{dp} \left(\frac{\vartheta dp}{\varepsilon x \upsilon}\right) 0.72$$

Modifying equation 9 from Reference 1 (p. 365).

$$Km = \frac{\vartheta}{ah} \ln\left(\frac{Co}{C_h}\right) \text{ (Please refer to Figure)} \quad (5)$$

[h is length through which electrolyte flows in the electrode bed.]

h = 0.1 m
Co = inlet concentration of reacting species, moles/m^3
C_h = outlet concentration of reacting species, moles/m^3

$$\therefore \ln\left(\frac{Co}{C_h}\right) = \frac{ahKm}{\vartheta} \quad (6)$$

$$= 66 \text{ to } 15$$

This indicates that under limiting current conditions, Ch << Co or in other words we will have close to 55-100% conversion. Under these conditions, total current

$$I = nFQ(Co-Ch)$$
$$\cong nFQ(Co) \times conv. \quad (7)$$

Let C_T = concentration of all Cobalt species

$$\text{and } \chi = \frac{L - Co^{3+} \text{ moles present}}{\text{Total of Co present}} \quad (8)$$

$$\text{Concentration of } L - Co^{3+} = \chi C_T \quad (9)$$

$$\text{and } (L - Co^{2+})_2 - O_2 = \frac{1-\chi}{2} \cdot C_T \quad (10)$$

Footnote 1 continued In our case this leads to:

$Km = 2.3\ 10^{-6}$ to $1.1.10^{-5}$ for ϑ = 2 to 18 mm/s

Using these values,

$$\ln\frac{Co}{C_h} = \frac{a\ h\ Km}{\vartheta} = 1.5 \text{ to } 0.79$$

$$\frac{Co}{C_h} = 4.5 \text{ to } 2.2$$

which implies 78 to 55% conversion for the two velocities.

This is roughly what we got in experiment 1KS40.

Free L - Co^{2+} is assumed to be negligible at the anode inlet, as it is fully oxygenated.

Equation 7 can be converted to yield limiting current density over the separator area (refer to Page 43).

$$i = I/wh = \frac{nFQCo}{wh} \text{ x conv.} = \frac{nF\vartheta \cdot Lw}{wh} Co \text{ x conv.}$$

$$= \frac{nF\vartheta L}{h} Co \text{ x conv.} \qquad (11)$$

where Q is total flow rate.

Cathodic limiting current

$$i_{c,L} = \frac{F\vartheta L}{h} C_T \chi \text{ x conv.} \qquad (12)$$

Anodic limiting current

$$i_{a,L} = \frac{F\vartheta L}{h} (1-\chi) C_T \text{ x conv.} \qquad (13)$$

For $\chi = 0.2$, $\vartheta = 2.10^{-3} - 18.10^{-3}$ m/s, conv. = 100%

$$i_{c,L} = 772 \text{ A/m}^2 - 6948 \text{ A/m}^2$$
$$i_{a,L} = 3088 \text{ A/m}^2 - 27792 \text{ A/m}^2$$

We will consider the high velocity operation (18 mms^{-1}) where we normally operate at 450 A/m^2. This reflects that we are well below mass transfer limiting conditions at this operating point.

3. Kinetic and Ohmic Loss in the Porous Bed:

The voltage drop in the porous bed is conveniently given by Ref. 2, p. 31, equation 43 for linear polarization.

(Average true current density on felt fibers = 450/66 A/m^2 = 6.8 A/m^2, exchange current density is reported to be 13 A/m^2, since operating current density is lower than exchange current densities, linear polarization case can be construed to be accurate. 66 is the area enhancement due to felt.)

$$\phi_1(L) - \phi_2(o) = \frac{Li}{\kappa+\sigma} \left[1 + \frac{2(\frac{\sigma}{\kappa} + \frac{\kappa}{\sigma})\cosh \mu}{\mu \sinh \mu} \right]$$

where $\phi_1(L) - \phi_2(o)$ is voltage loss

κ is effective electrolyte conductivity

σ is effective solid matrix conducticity

μ^2 is $(\alpha a + \alpha c)\frac{FaioL^2}{RT}\left(\frac{1}{K}+\frac{1}{\sigma}\right)$

αa, αc are transfer coefficient

io is exchange current density

$\frac{F}{RT}$ is $(0.059 \text{ volt})^{-1}$

$\kappa_{anolyte} = 20\ (1\text{-}0.11)^{1.5} = 16.8\ Sm^{-1}$ from Bruggeman-Maxwell equation

0.11 is (0.06) carbon + gas (0.05 average) volume fraction

$\kappa_{catholyte} = 20\ (1\text{-}0.06)^{1.5} = 18.2\ Sm^{-1}$

$\sigma = 400\ Sm^{-1}$ (measured, Sam Mohanta)

$a = 1.32.10^4\ m^{-1}$ (measured, E. De Castro)

$io = 13\ A/m^2$ (measured, E. De Castro)

$\alpha a + \alpha c = 1$ (from E. De Castro)

$L = 0.005m$

The above relationship yields,

voltage drop = 0.00015 i where i is current density in A/m^2

4. Other Losses

   A. Contact loss between current collector and felt:

      We have measured contact resistance using Ti and Graphite as current collectors with the following variations:

      1) Wet with salt solution and dry felt,
      2) Graphite and two sources of Ti
      3) Compression of felt

The experimental cell has a contact resistance between one electrode and felt of $0.5.10^{-4}$ to 1.10^{-4} ohm-m^2.

In cases when $K<<\sigma$, $\mu>2$

$$\phi_1(L) - \phi_2(O) = \frac{Li}{\kappa\mu}$$

$$= \frac{i}{\kappa^{1.5}} \sqrt{\frac{RT}{Faio(\alpha a + \alpha c)}}$$

This means L has no bearing on the voltage drop. This is somewhat interesting.

B. Separator:

Aquanautics uses Celgard hydrophillic microporous separators of 0.001 in. or 25.4 μm thickness, 40% porosity. The electron micrograph shows the pores are straight through. Therefore, the resistivity

$$= \frac{25.4 \,.\, 10^{-6} m}{\kappa \times \text{porosity}}$$

$$= 3.2 \times 10^{-6} \text{ ohm-m}^2$$

5. Summary

The losses are therefore:

	Resistance 10^{-4} ohm-m^2	mV loss at 450 A/m^2
1. Felt & Ti @ anode	0.5 - 1	22.5 - 45
Felt & Ti @ cathode	0.5 - 1	22.5 - 45
2. Kinetic + ohmic through		
felt @ anode	1.5	67.5
Felt @ cathode	1.36	61.2
3. Separator	0.032	1.4
4. Thermodynamic	-	120
		295 - 340 mV

Observed: Expt. 3VLC56g, 450 A/m^2 286 mV

References:

1. John S. Newman, William Tiedemann, Adv. in Electrochem. and Electrochem. Engg., vol. 11, Wiley. "Flow-Thru Porous Electrodes", p. 353 - 438.

2. John Newman and William Tiedemann, Porous Electrode Theory with Battery Applications, AICHE Journal (Vol. 21, No. 1) Jan. 1975, p. 25-41.

3. K. Kinoshita and S. C. Leach, Mass Transfer Study of Carbon Felt, Flow-Through Electrode, J. Electrochem. Society, p. 1993 - 1997, vol. 129, no. 9, 1982.

2.B Scale-up with ABC-250 (4-cell Monopolar Stack)

Objective

The objective of this experiment was to examine the performance of a newly built four-cell monopolar stack constructed using Aquanautics' design designated the ABC-250. This experiment was designed to measure the current density, oxygen output and purity as well as the specific power consumption of the four-cell stack using a standard carrier solution for comparison with EOC data. The extent to which the performance scaled up from an EOC to a cell 40 times larger in area was to be quantified.

Background

Prior to this experiment the Aquanautics cell had only been tried a few times. First experiments with a prototype unit used graphite electrodes that were porous and leaked carrier. Those experiments were conducted in one cell stacks and the cell performance scaled up linearly with that observed on an EOC scale as well as on an MP cell scale. The Corporate Objective run was the first use of the Aquanautics cell in a stack and resulted in external as well as internal leaks due to faulty glue joints in the frame as well as bad assembly practises. After that experience a one cell stack was built with repaired frames and with titanium current collectors for the NASA demonstration unit. This unit worked well, without leaking, though its performance characteristics were not calculable due to unloader inefficiencies. Buoyed by this a four-cell stack was constructed for testing with a huge unloader to overcome any problems there may have been with the unloader design.

Experimental Set-up

The experimental set-up is shown in Figure 1.

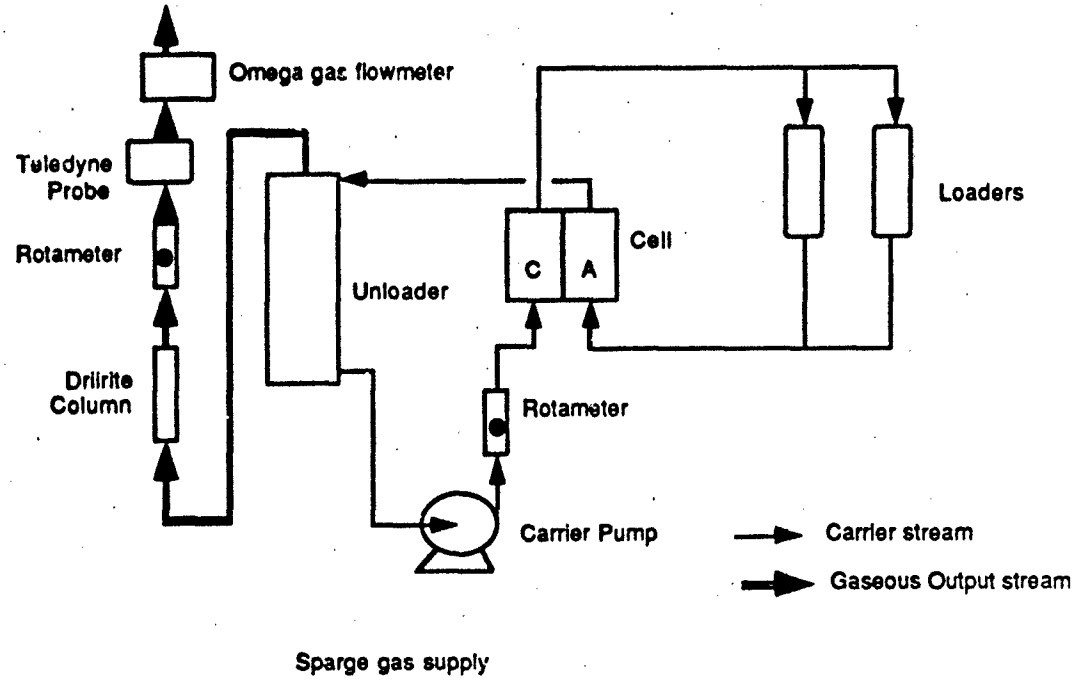

Figure 1

The different components were hooked up together as shown in the diagram. The cell stack was constructed with titanium current collectors, VDG carbon felts as the cathode and Ultracarbon felts as the anode. Celgard 3400 hydrophillic membranes were used as the separator in the cell stack. Loading was affected by means of a couple of Hoechst-Celanese hollow fiber modules offering a total surface area of 5.6 m^2. The unloader was a sparge tower of inner diameter of 76 mm and a length of 610 mm. Sparging was not used and the ports for entry of sparge gas were blocked off. Pure oxygen was collected over a pool of carrier in the tower and the flow and purity of the output measured by a rotameter and a Teledyne oxygen probe respectively. A Micropump centrifugal pump was used for carrier circulation, and a Gilman rotameter used to measure and set the rate of carrier flow. The carrier used was a 0.4 M solution of Compound #64 in a freebase form with 3.5 M KCl as the supporting electrolyte. The Catalyst used in this experiment had a concentration of 8 mM.

Procedure

The experiment was started by inserting the carrier into the system and letting it oxygenate for an hour or so. Power was turned on and the cell potential set at 0.5 V. The carrier flow rate was set at 2600 ml/min initially (corresponding to a specific flow rate of 26 l/min/m^2). The flow rate was then reset to 1300 ml/min (13 l/min/m^2) after an hour or so and the experiment continued at this setting. After a day had elapsed the cell potential was turned down to 0.3 V and the experiment continued for another day until the carrier stopped

putting out appreciable quantities of oxygen in spite of consuming large currents. At this point the experiment was discontinued.

Results

The results of this experiment are presented in the form of four graphs shown in Figures 2 through 5. Figure 2 shows a plot of the oxygen output from the system as a function of time. This plot identifies a peak output of 240 ml/min of oxygen. Figure 3 is a plot of the specific electrochemical power consumed to produce oxygen as a function of time also. Figure 4 shows the purity of the oxygen as observed by the Teledyne probe over the entire span of the experiment, while Figure 5 is a history of the fractional conversion achieved in the electrochemical cell.

Conclusions and Discussion

Figure 2 shows th·: a peak oxygen production of 240 ml/min was achieved at 0.5 V and a carrier flow rate of 13 l/min/m^2. The EOC has been shown to put out about 6 ml/min of oxygen with the same carrier and under the same conditions (4VLC13). Since a four cell stack of the Aquanautics' design has an area of 1000 cm^2 or approximately 40 times greater than the EOC, this was considered proof of scale-up without loss of efficiency.

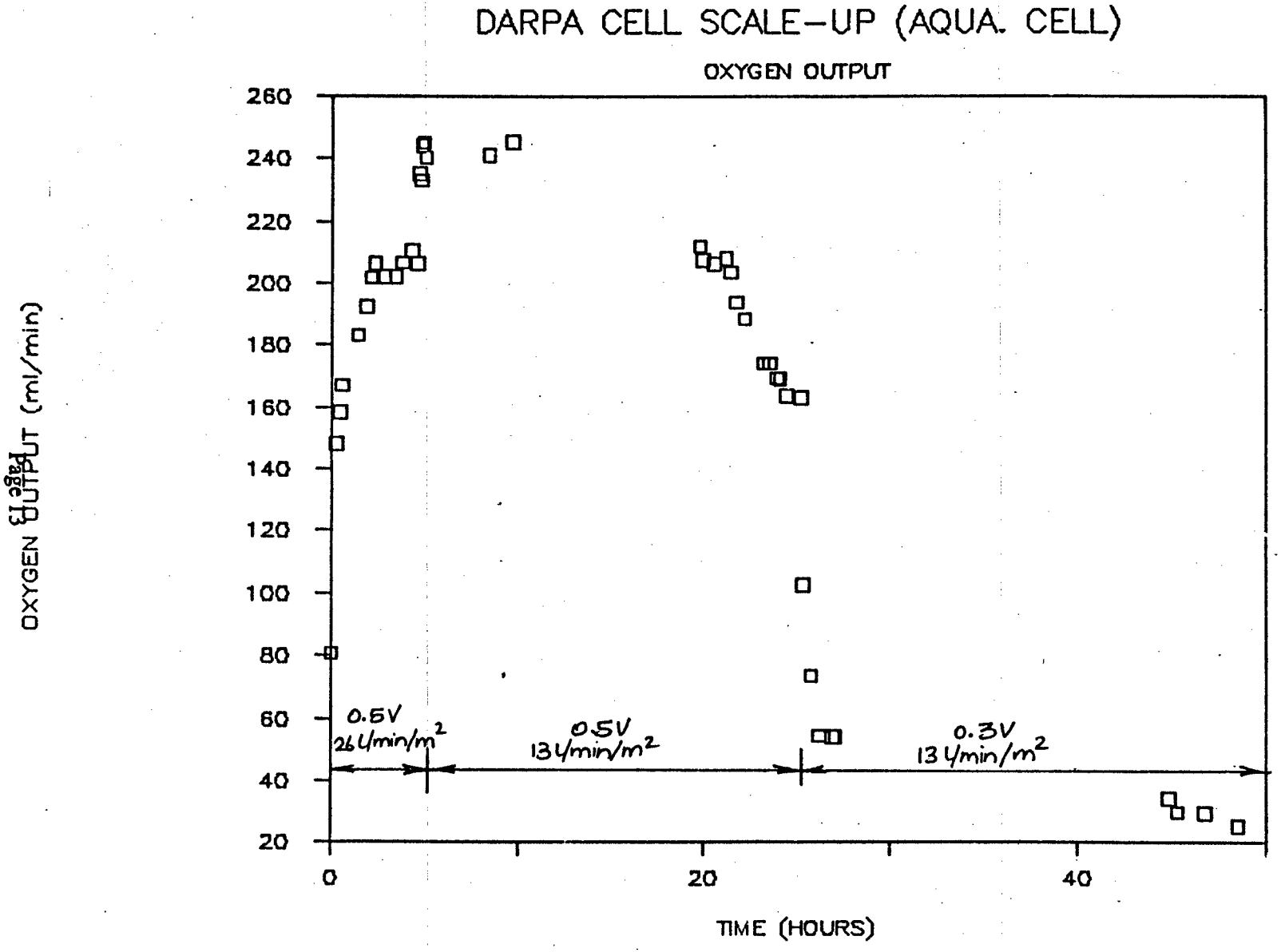
DARPA CELL SCALE-UP (AQUA. CELL)
OXYGEN OUTPUT
OXYGEN OUTPUT (ml/min)
260
240
220
200
180
160
140
120
100
80
60
40
20
0
20
40
TIME (HOURS)
0.5V
26 l/min/m²
0.5V
13 l/min/m²
0.3V
13 l/min/m²

Figure 2

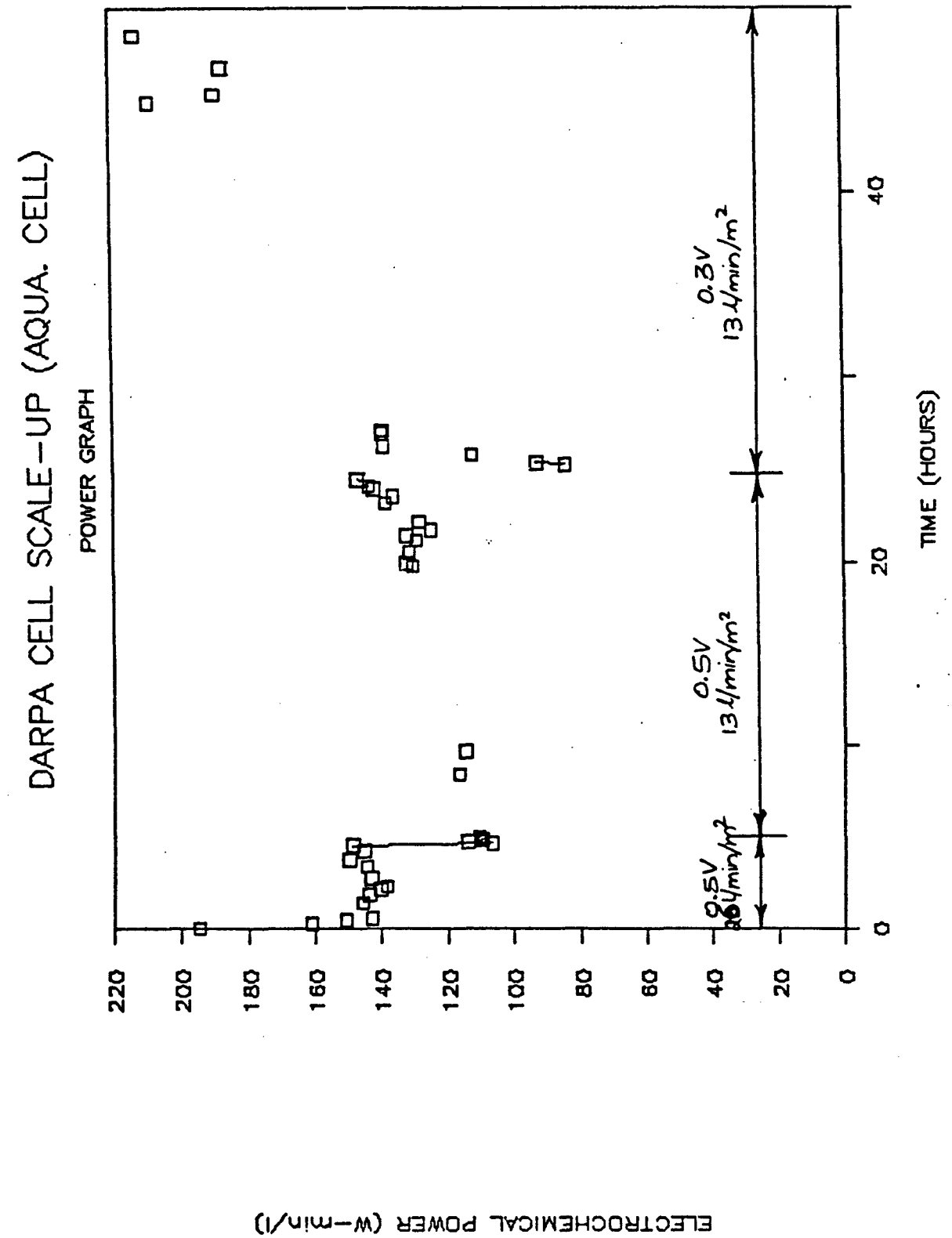
DARPA CELL SCALE-UP (AQUA. CELL)
POWER GRAPH
ELECTROCHEMICAL POWER (W-min/l)
TIME (HOURS)
0.3V
13 l/min/m²
0.5V
13 l/min/m²
0.5V
20 l/min/m²
220
200
180
160
140
120
100
80
60
40
20
0
0
20
40

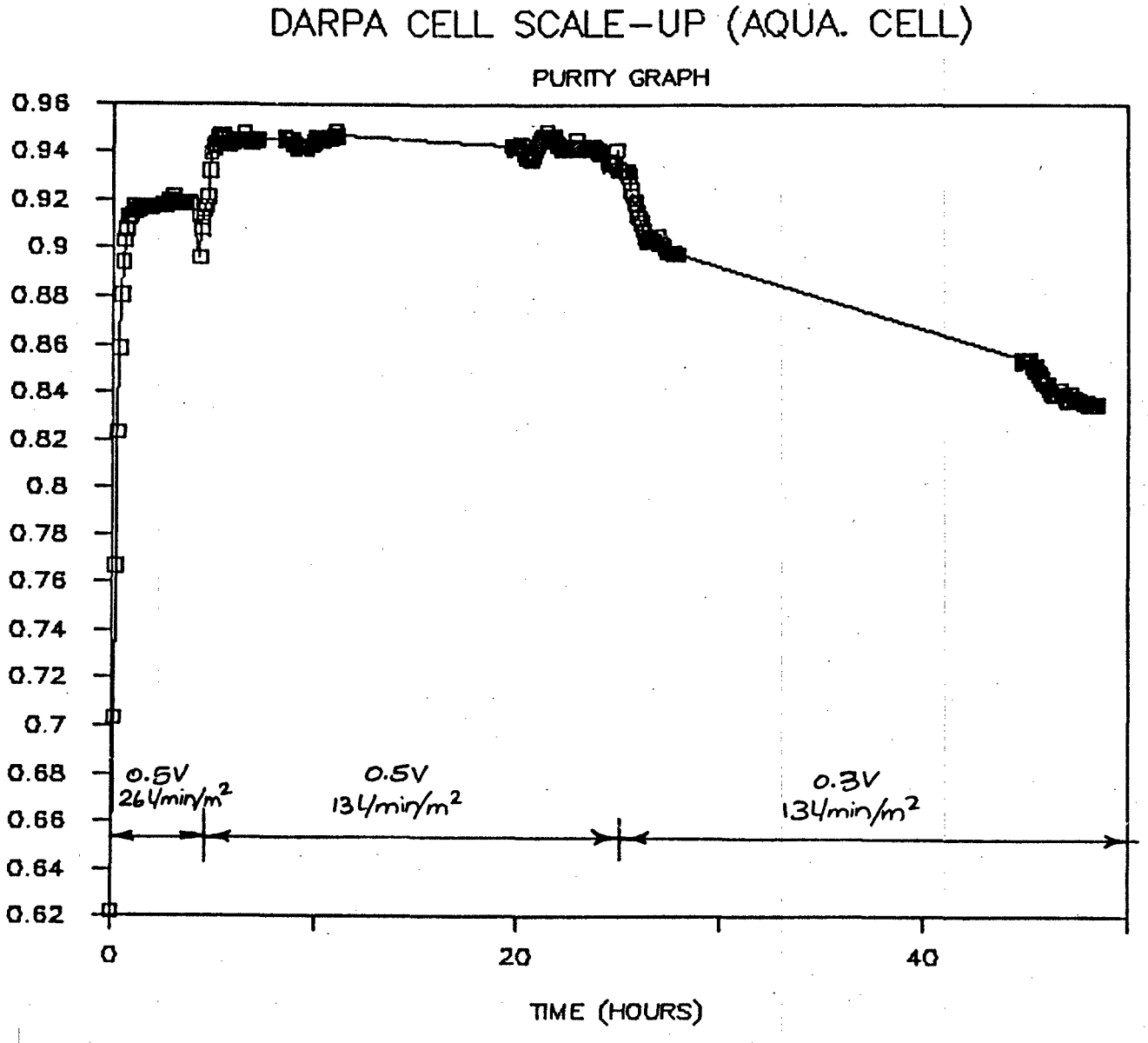
DARPA CELL SCALE-UP (AQUA. CELL)
PURITY GRAPH
OXYGEN PURITY
0.96
0.94
0.92
0.9
0.88
0.86
0.84
0.82
0.8
0.78
0.76
0.74
0.72
0.7
0.68
0.66
0.64
0.62
0.5V
26 l/min/m²
0.5V
13 l/min/m²
0.3V
13 l/min/m²
0
20
40
TIME (HOURS)

Figure 4

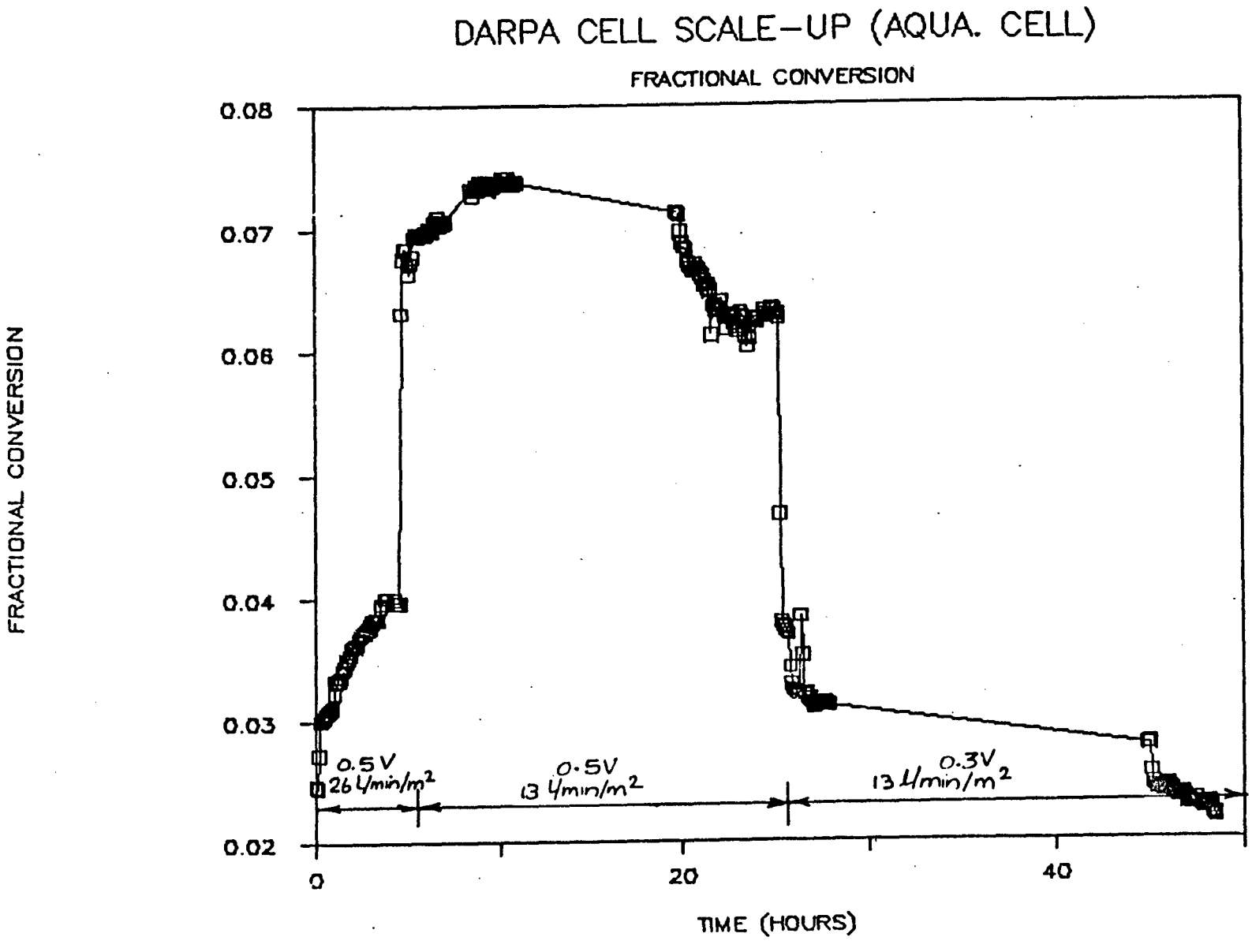
DARPA CELL SCALE-UP (AQUA. CELL)
FRACTIONAL CONVERSION
FRACTIONAL CONVERSION
0.08
0.07
0.06
0.05
0.04
0.03
0.02
0.5V
26 L/min/m²
0.5V
13 L/min/m²
0.3V
13 L/min/m²
0
20
40
TIME (HOURS)

Figure 5

2.C Scale-up with ABC-250: Monopolar vs. Bipolar

Objective

The objective of this experiment was to compare the performance of a five-cell monopolar stack with a five-cell bipolar stack. The stacks were both made from the Aquanautics cell designated ABC-250. The purpose of the experiment was to subject both stacks to the same set of conditions and evaluate performance using the same carrier to eliminate any differences that tend to arise when the carrier is made in separate batches. The performance of each stack was evaluated in terms of the power-output and the cell voltage-current relationships.

Background

The Aquanautics cell was designed with bipolar operation in mind and accordingly attention given to arcane details of manifold and channel geometry. Prior to this experiment the design had only been tried in the monopolar mode for comparisons with the MP cell and the EOC and to establish process scale-up. The ABC-250 was then assembled in two seven-cell stacks, one monopolar in construction and the other bipolar. Preliminary characterization studies were done using a 0.1 M solution of Ferrous Chloride and Ferric Chloride to evaluate the difference between the conversion efficiencies of the two stacks. These experiments are described in the laboratory books of Dr. De Castro and Mr. Shrinivasan (lab book designations 9ED26, 1KS34, 1KS36, 9ED36, 1KS39, and 9ED45). The characterization studies showed that the bipolar stack had a few cells that exhibited large potential drops. Comparison with the monopolar stack using the conversion rate as measured by an ORP were inconclusive due to the unreliability of the ORP data. Hence the comparison was done using the Aquanautics process where conversion could be measured in terms of a tangible output, in this case oxygen.

Experimental Set-up

The experimental set-up for this study is shown in Figure 6.

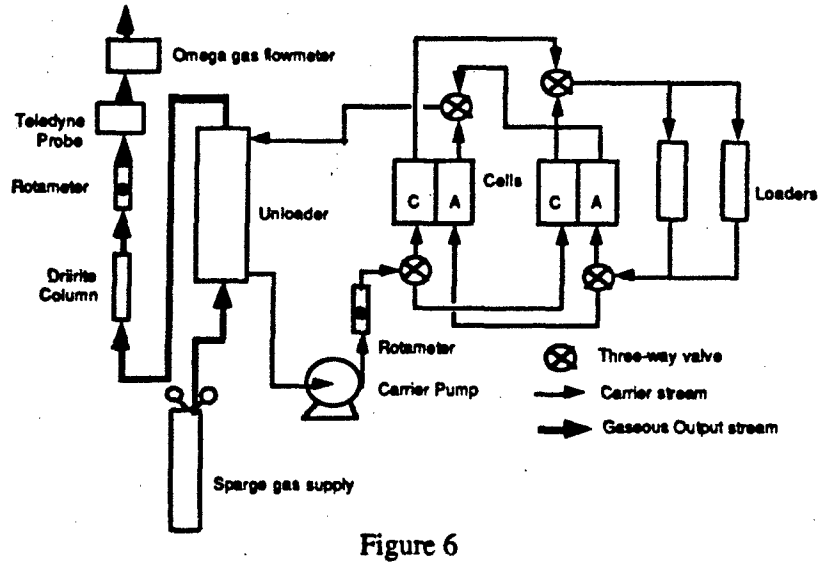

Figure 6

Procedure

The bipolar and monopolar stacks were connected into the carrier loop as shown in Figure 6. Prior to this they were flushed of all the ferrous/ferric chloride that has been used for preliminary evaluation. The cells were then rinsed with 1 M hydrochloric acid and then deionized water. The cell stacks shared the unloader, loader, carrier pump, rotameter and oxygen product stream components. The cells were activated or switched into the carrier stream by using a combination of four three-way valves as shown in Figure 6.

Both cells were assembled with titanium current collectors and VDG carbon felts as the cathode and Ultracarbon felts as the anode. Celgard 3400 hydrophillic membrane was used as the separator. The carrier used for this study was a 0.4 M solution of compound #64 which contained 3.5 M KCl as the supporting electrolyte and 8 mM DAMF as the catalyst. Two Hoechst-Celanese cartridges were used for loading and the unloader was a 76 mm inner diameter, 610 mm long PVC column with Nitrogen as the sparge gas. The total loader surface area was 5.6 m^2.

During the preliminary evaluation studies it was determined that the last two cells in the monopolar stack had been damaged and were no longer working properly. It was therefore decided that evaluation using carrier would have to be done with two cells idling in both stacks. This meant that though carrier was flowing through the cells, power was not applied.

The first run was made with a carrier flow rate of 1.1 l/min which corresponds to a specific flow rate of 6 l/min/m^2. The first five cells of both the monopolar and bipolar stacks were connected to separate power supplies. The voltage and current for both stacks were monitored using a Scientific Solutions board and an IBM PC. The output flow rate and purity were monitored using an Omega flow meter and a Teledyne probe respectively. Four sets of readings were taken for both stacks. These readings were at average cell potential of 0.3, 0.37, 0.44, and 0.5 volts. The cells were operated in an alternate fashion at these potentials so that better mixing of carrier and therefore more complete equalization of conditions achieved. The bipolar stack revealed that the first cell was experiencing a large potential drop and therefore the readings with the bipolar stack was repeated by applying the stack potential to the middle five cells in the stacks and thus eliminating the malfunctioning cell. Therefore two sets of bipolar readings were obtained, one using the cells corresponding to the active cells in the monopolar stack and the other using the five best cells in the stack.

The experiment was repeated the next day with oxygen output being measured for both stacks at three cell potentials, 0.3, 0.37, and 0.5 volts. Other conditions remained the same as before, except that the carrier was a day older.

Results

The results of this comparison are presented in Figures 7 and 8. Figure 7 shows the plot of cell current as a function of the cell potential for all experiments. Figure 8 shows a plot of cell output as a function of electrochemical power.

Figure 7

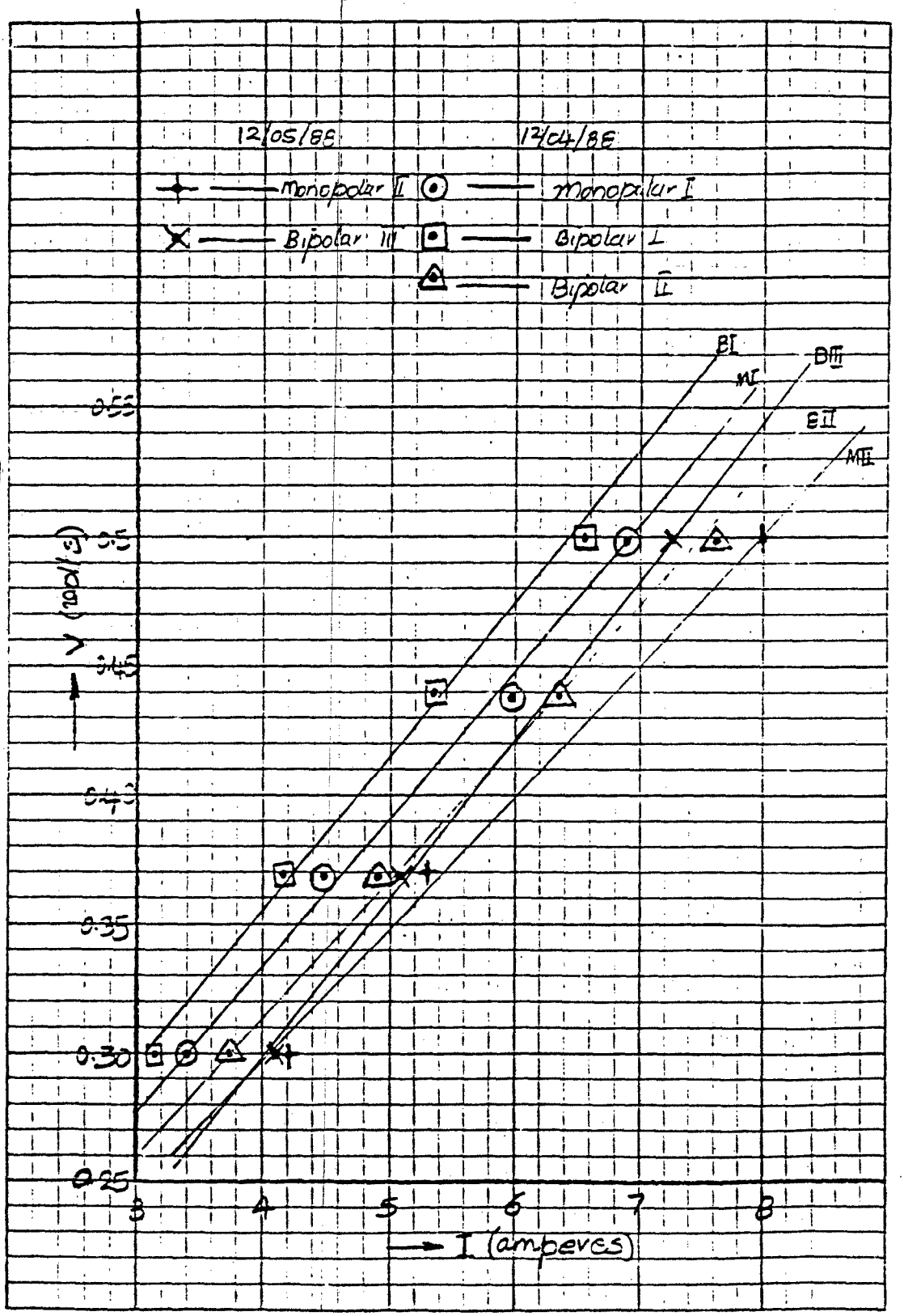
12/05/88
12/04/88
Monopolar II
Monopolar I
Bipolar III
Bipolar I
Bipolar II
BI
MI
BIII
EII
MII
0.55
0.50
0.45
0.40
0.35
0.30
0.25
γ (Ω/cm)
3
4
5
6
7
8
I (amperes)

Figure 8

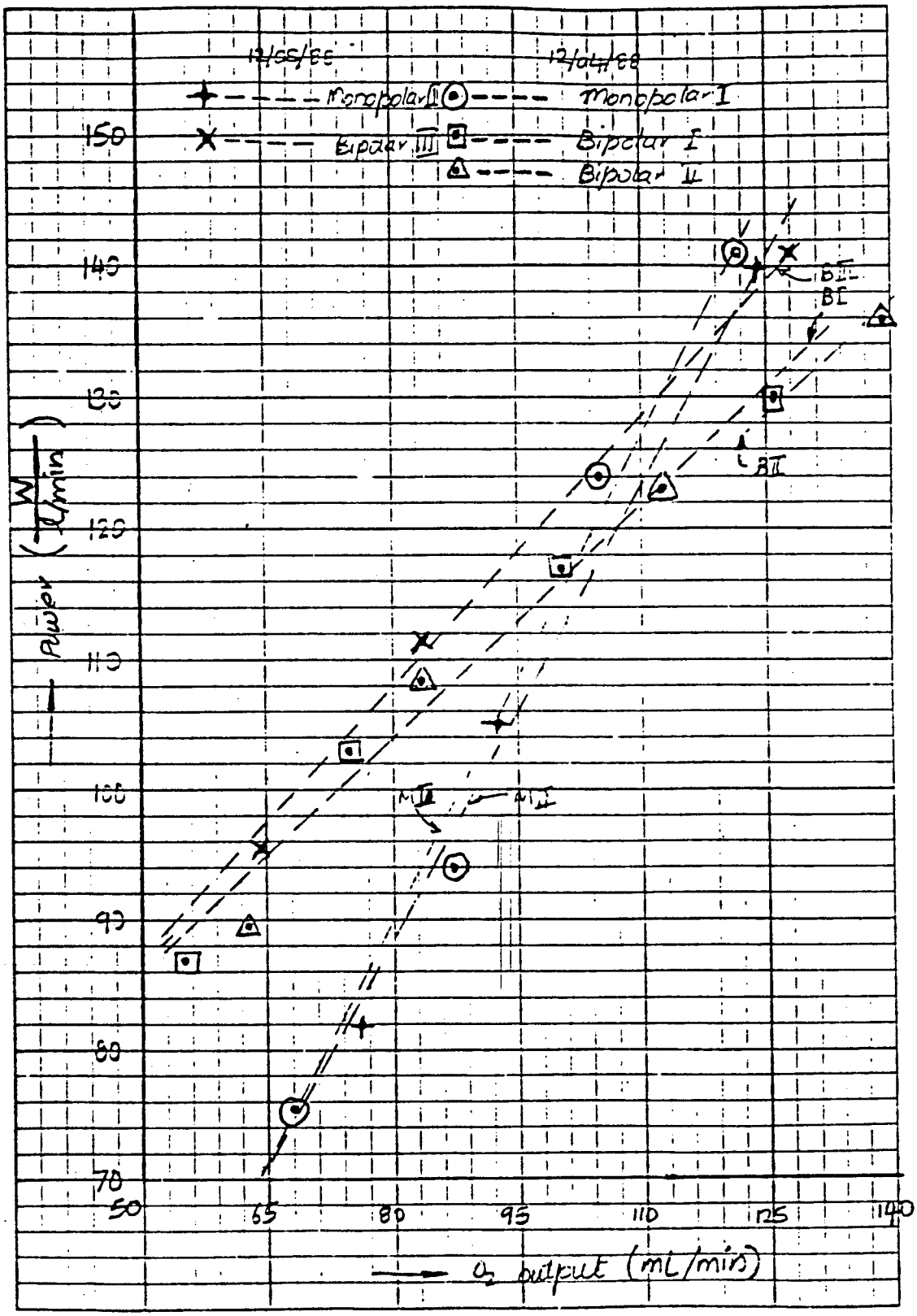
12/55/88
12/24/88
Monopolar II
Monopolar I
Bipolar III
Bipolar I
Bipolar II
150
140
130
120
110
100
90
80
70
50
65
80
95
110
125
140
BI
BII
MI
MII
Power (kpm/min)
O2 output (mL/min)

Conclusions and Discussion

Figure 7 shows that the current-voltage characteristics of both the stacks as measured at different times. Bipolar I refers to the run where the cells corresponding to the active ones in the monopolar stack were energized (cell #1 through #5). Bipolar II refers to use of the middle five cells in the stack which were determined to work the best. Both these runs were performed on the first day (12/04/88). Bipolar III refers to the experiment done on the second day (12/05/88). Monopolar I refers to the monopolar run performed on the first day and Monopolar II to the test on the second day. It is obvious that the current-potential relationship for both stacks are similar within experimental error. Most of the experimental error could be located at the shunt used with the bipolar stack power supply. The shunt was a 2 mohm resistance which provided a very small potential drop for the data acquisition system to monitor. The resolution of the current measurement could have therefore contributed to most of the experimental error.

Figure 8 shows the output-specific power relationship. The interesting observation to be made here is that the monopolar stack performs better than the bipolar stack at low specific powers (corresponding to lower cell potentials), while the latter works better at higher potentials. The crossover of performance curves seems to occur approximately between specific powers of 115 W/l/min and 135 W/l/min. These results are to be confirmed by repeating the experiment with newly rebuilt stacks of cells at a later date. The output of both stacks were not as high as expected and the electron counts were high. This may be due to the nature of the carrier which was in its freebase form and also the damage that the cells may have sustained in their preliminary testing with ferrous and ferric chloride.

2.D Gill

Objective:

1. To develop a gill system for deep seawater oxygen extraction using membrane technology.
    - The system must withstand operating conditions of up to 6,000 meters of ocean depth.
    - The total volume of the gill should be no larger than 80 liters per liter per minute of delivered oxygen.
    - Oxygen flux should not deteriorate more than twenty percent over two years.
    - Seawater pumping costs should not increase more than ten percent over two years.
2. To provide a gill system for 10W demonstration.

Work Carried Out:

1. Identify membrane materials and existing membrane packages.
2. Literature search for evidence of fouling at depths greater than 700 meters.
3. Membrane testing device designed and built.

1. Membrane Search:

We have contacted various membrane and membrane package manufacturers. These companies and their products are described in Table 1. The companies which produce only microporous membrane are discounted for very deepsea application. Between hollow fiber membrane and sheet membrane types, the former provides the best space-time yield. Therefore this type is given the top priority to be pursued.

Table 1

Name of Company	Microporous Only	Solid Membrane		
		Sheet	Fiber	Packaged
Advanced Membrane Technologies			x	x
Biodynamics	x			
CD Medical (DOW)	x			
DOW USA*				x
Filmtec (DOW)	x			
GTF (Le Carbone Lorraine)		x		
Gelman Sciences	x			
Hoechst Celanese	to be checked out for custom design			
Innovative Membrane Systems*				
KOCH Membrane Systems	x			
Membrane Technology & Research		x		
Sci Med Life Systems		x		x
UBE		x		x
Mitsubishi-Rayon			x	x

* Won't sell.

Three membranes have been identified as potential materials for the gill.

Advanced Membrane Technologies	Hollow fiber microporous membrane with silicon coating.
Membrane Technology Research	Flat sheet composite silicone membrane with polyester support.
Sci Med Life Systems	Flat sheet silicone membrane with a nylon support.

Membrane evaluation will be based on oxygen flux, fouling studies, and ultimately depth capability.

2. Fouling related goals are as follows:

- Oxygen flux should not deteriorate more than 20% over a period of two years, and
- Seawater pumping costs should not increase more than 10% over a period of two years.

Literature study on fouling shows that there could be two types of fouling:

1. Biological
2. Geological

Biological Fouling:

Microorganisms like bacteria lead to macroorganisms like algae and barnacles via diatoms, fungi, microalgae and protozoa. These may lead to cnsiderable increase in the resistance of oxygen transfer and/or seawater pumping.

Figure 9 shows bacteria counts and diatom growth as a function of depth. Figure 10 shows that for plankton biomass. It is therefore postulated that biological fouling on the ocean bottom will be minimal. The various readings on sunken ships such as the Titanic also corroborates the above deduction.

Geological Fouling:

The other form of fouling will be suspended solids like mud, silt and sand in water. There is a considerable amount of this on the sea bottom. The system would need to be positioned accurately, the gill design needs to take into consideration this fact and system design might need to include occasional cleaning, simulating a fish operating its own gill.

A full literature report is scheduled to be completed by the end of this month.

Plan:

1. Oxygen Flux Measurements

   Determine the rate of oxygen flux from seawater to carrier:

   @ Zero degrees Celsius
   @ Matched carrier and seawate: vapor pressures
   @ Different seawater oxygen contents.

   With different types of membranes, using Celgard 2400 microporous membrane as a control.

2. Pressure Testing Measurements

   Test the integrity of the membrane to pressure breakthrough by checking the effects of taking a membrane to 9000 psi with carrier on one side and seawater on the other.

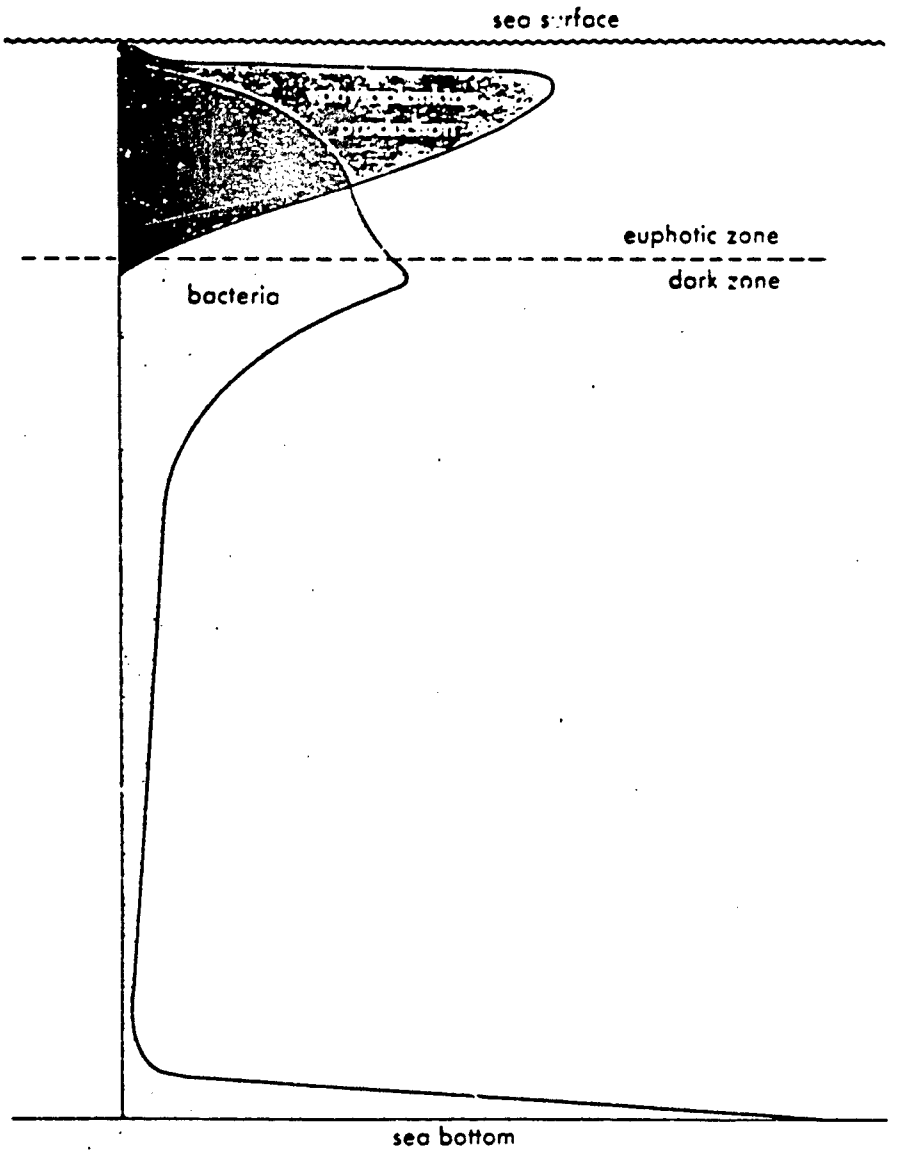

Figure 9 Distribution of decomposer-bacteria in the open sea. Very high bacterial counts are found immediately below the levels of maximum diatom growth, the numbers fall off in the intensely illuminated surface waters and also in intermediate depths, and the greatest counts are found at the surface of the bottom deposits. (Reference: W. D. Russell-Hunter, Aquatic Productivity, p. 170, MacMillan Company, 1970)

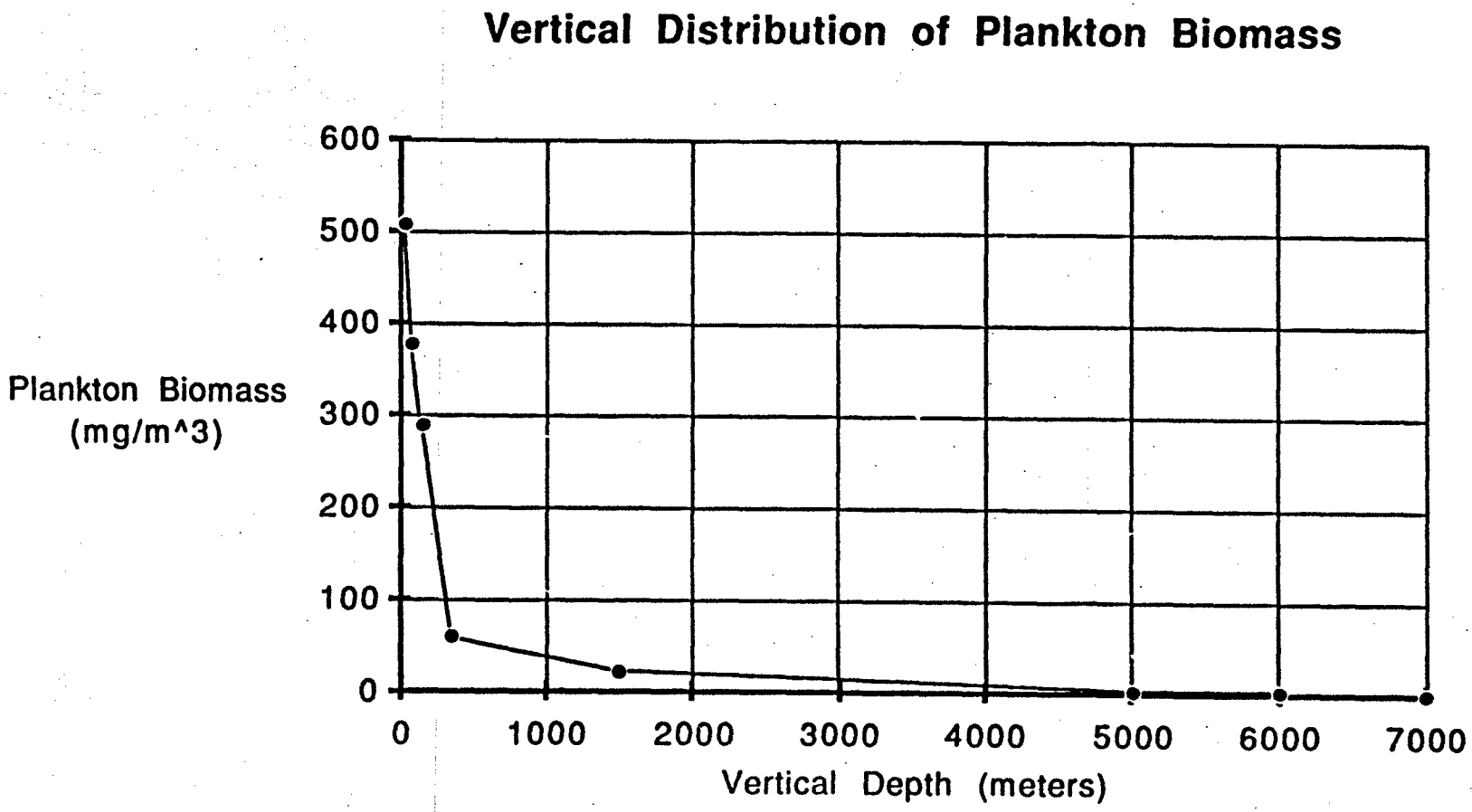
Vertical Distribution of Plankton Biomass
Plankton Biomass (mg/m^3)
600
500
400
300
200
100
0
0
1000
2000
3000
4000
5000
6000
7000
Vertical Depth (meters)

Figure 10

3. Technological Progress

Two areas of the technology, longevity and kinetics, are vital to the Aquanautics technology. The 'target' design points for UUV (Unmanned Underwater Vehicle) or UPS (Underwater Power Sources) are as follows:

	UUV	UPS
Carrier Longevity	> 3 months	> 1 year
Kinetics:		
Cell Output - lpm O_2/m^2	1	1
@ sp. power - w/lpm O_2	25	25

Achieving these design points would make Aquanautics technology 2-5 times better than the stored O_2 option.

In the following sections, work related to longevity and kinetics are described.

3.A Carrier Longevity

Aquanautics is working towards discovering or inventing a new longer life carrier. In collaboration with the University of California, Davis, we are formulating and synthesizing small quantities of new compounds at a rate of 2/month. These compounds are then screened and approximately 2 compounds per month are selected for producing larger quantities. These are then tested in electrochemical flow cell. There have been 4 such compounds tested this quarter in the electrochemical flow cells. There are also 12 such compounds ready to be tested.

3.A.1 Screening and Carrier Degradation

Abstract

The fourth quarter of 1988 research results is summarized. A new procedure for the rapid screening of new carriers has been worked out. Measurement of oxygen uptake by using a Clark type oxygen probe was found to be very accurate even when a single oxygen concentration was used (a one point determination). Another procedure using a oxidation/reduction probe was found to be very inaccurate and therefore eliminated. The analysis of EOC solutions for degradation products has continued but without much success.

Introduction

During the last quarter, much progress has been made. The Army SBIR work has shown that the Aquanautics oxygen extraction technology can be made to work in atmospheres contaminated with cyanide and carbon monoxide. The later is a very significant finding from the standpoint of a producing a portable oxygen system for medical applications.

A new screening procedure has also been worked out. The previous method was a more rigorous procedure that required at least a week for a single compound. The method makes use of semi-quantitative procedures. It is now possible to obtained solubility, purity, oxygen affinity and, cyclic voltammetry in *ca.* 2 days per compound. If this method is used then the back log of carrier screening will be transferred to the EOC's.

Little progress was made in degradation studies. The procedure for the removal of the cobalt from EOC solutions still has not been worked out. However, it was possible to extract some organic components from an EOC solution. GC/MS data was obtained on these compounds.

3.A.2 Electrochemical Testing of the Carriers

Summary

We have demonstrated in separate carriers the necessary properties for successful commercialization of the technology: Lifetime greater than one month; fast oxygen release kinetics; high fractional conversions; high current efficiencies and low power capabilities. The knowledge is still being assimilated and our experimental methods are still evolving to meet the new requirements. Construction of new EOCs is underway and the project is on time and under budget. Present rate of screening is more than twice the rate committed to with Liquid Air and this rate will increase further. The 2'-Laura-methyl series was completed and despite some irreproducibility, a definite difference in the failure mode was distinguished from the Suzy series. No catastrophic rise in the electron count number was observed. Rather the carrier's performance simply 'faded' away. Both current and output decay to unmeasurable levels. An explanation is proposed. Three new EOCs have been built and tested. Pump problems remain and the unloader efficiency for pure oxygen output is still under study.

Objectives

1) To screen at least one new compound per month.
   Status: completed
2) Complete installation of new EOCs
   Status: completed except for new pump installation
3) Optimize carriers already in hand with respect to effects of impurities on longevity and output level.
   Status: ongoing
4) Design new simplified EOC equipment in conjunction with L'Air Liquide.
   Status: on hold until negotiations complete

Results and Discussion

33SP

The mode of failure of this carrier is illustrated in Figures 11 and 12 which show the behavior of the electron count with time. This behavior comes from the rapid decrease in the oxygen output while the current declines at a much slower rate. The lifetime of the carrier is only 50 hours where the electron count is below 4. This particular experiment was performed in the constant voltage mode. An almost identical electron count-time profile was observed when the carrier was operated in the constant current mode. The failure can also be detected in this mode by the increase in cell voltage. Such a voltage rise could be used to indicate carrier failure in the commercial device and the circuitry could then sound an alarm.

Experiments have been carried out with th is carrier where the effect of the electrode bed depth was examined (Experiment No. 4VLC17). From the current profiles it appears that reducing the thickness of the cathode has a greater effect on the current than reduction of the anode thickness. The effect seems to be even more pronounced on the oxygen output. However, it can be seen that the changes in thickness were carried out while the carrier failure was beginning to accelerate. The electron count time profile is unaffected by the bed depth changes. It seems that the cathode may well be limiting particularly with respect to the oxygen release but the carrier instability makes it difficult to draw firm conclusions.

It is clear that it is not worthwhile to try to do the bed depth experiments with a carrier like 33SP as its lifetime is too short. One theory has been put forward to account for the increase in the electron count is that the ligand is deprotonated to form the imine and that the imine then decomposes over time to form complexes which take up current but which do not release oxygen as a result of that current. Thus the behavior of 33 SP Imine should be similar to 33SP.

33 SP Bis Imine.

Results from this carrier were somewhat irreproducible. An initial experiment showed carrier failure after 16 hours but three other experiments showed reasonable lifetimes which are exemplified by 4VLC19. The electron count, power and outputs all look fairly similar to 33SP so the theory that the imine is the product of the degradation of 33SP is not contradicted by the results. The interesting point to note is that the complex formation between the imine and cobalt apparently stabilizes the imine bond which is normally very unstable in water.

23SP

This compound has shown surprising stability. Three experiments have now been run where the carrier has lasted for more than 30 days. The longevity criteria have been formulated with this carrier. They are the length of time that the electron count remains stable while the oxygen output remains at a meaningful level (0.5 ml/min). The behavior is shown in Figures 11 and 12. The cell current and output are only a quarter of the initial values but the electron count and power (150 watt.min/l) remain relatively constant for about 28 days before the familiar failure mode begins to set in. The values obtained towards the end of the experiment are more inaccurate due to the small amount of oxygen produced. During the course of the experiment the cell was periodically rebuilt with fresh separator or felts or cleaned by rinsing with HCl solution after which the original current and output would be partially restored. This indicates that some impurities may be fouling the surface of the electrode and separator and therefore some effort should be put into carrier purification to obtain higher output levels.

22SP

Considerable work was carried out on this carrier in conjunction with the NASA SBIR. Steady state data for that experiment was obtained for 40 hours with no sign of an increase in the electron count. A repeat experiment was attempted recently which suffered from a pump failure but the carrier lifetime before electron count increase was nearly one week (2JBK32z) without any cell rebuilding or cleaning. Rinsing of the cell restored the performance only briefly and the electron count rapidly rose to an unacceptable level. Incidentally, the latter experiment was carried out using the crude free base supplied by Regis. Another point to take note of is that DAMF does catalyze the performance, doubling the output at the same voltage without increasing the electron count.

Pure Suzy

Pure Suzy performed very poorly from a lifetime point of view as can be seen from experiment 4VLC26a. The electron count is initially very high and climbs even higher after only 30 hours of operation. This leads to suspicions that impurities in the crude suzy used at Beaufort may have been responsible for the long lifetime observed.

24SP

This carrier showed great promise on its first screening run at 0.1M concentration. Outputs of 0.5ml/min were observed at 30 watt.min/l using the Fedkiw cell. Catalysis with DAMF was also observed to be effective and the lifetime was longer than 33SP. Unfortunately the output dropped off to an unacceptable level after a week although the usual rise in electron count was not observed. An encouraging observation was that the electron count was in the region of 2.5 - 2.8. Unfortunately an increase in the concentration to .4M did not result in an increase in the oxygen output commensurate with concentration and the electron count was closer to 4. The carrier was not rigorously purified so impurities may account for this behavior. However an output of 1 ml/min at 60 watt.min/l with an electron count of 4 demonstrates that the 24 chain shows faster kinetics than 33SP.

33-2' Laura-Ben

The immediately obvious problem with this carrier was its solubility. The maximum usable concentration in the presence of supporting electrolyte was 50 mM. This was usable to determine the behavior of the carrier. The electron count was observed to be rather high (3.5) and the power requirement for 0.5 ml/min of output was 150 Watt.min/l.

Lifetime studies were also not encouraging with the electron count climbing to 6 very quickly. After 30 hours the solution was observed to turn bright red and the oxygen output was unacceptably low. It was also observed that DAMF had no catalytic effect.

33-2'-Laura-Me

The solubility of this compound was found to be acceptable since 0.3M concentration was achieved in the presence of 3.5M chloride quite easily. An initial screen at 50 mM showed encouraging results although it was again observed that DAMF had no catalytic effect. A 0.2M concentration run was carried out (4VLC27). Again the electron count was observed to be rather high (ca. 4). The lifetime run showed that the carrier lasted a good deal longer than the benzyl derivative, indicating that the benzyl group may have been cleaved in the previous experiments. The initial output at 0.7V is very good but the performance drops off quite rapidly. The electron count climbs slowly from an initially high value. Once again the indications are that impurities in the carrier may be responsible for the high electron count and the slow climb thereafter.

24-2'-Laura-Me

This carrier's initial performance at the 50mM level was outstanding. Fractional conversions at 0.6V were 12%, electron counts were 2 and output was >3ml/min. DAMF was shown to have a pronounced catalytic effect. The lifetime experiment was disrupted by an attempt to use a pure oxygen unloading system. Unfortunately, the unloader could not cope and large amounts of oxygen were swept into the cathode. When the air-sparge unloading system was restored the electron count was observed to have risen to 6-7, a value which was maintained for 170 hours before climbing. A second experiment with

50mM concentration was carried out for lifetime without DAMF and the electron count remained in the 2-3 range for 100 hours. The output dropped to a low level (0.4ml/min) which made it difficult to accurately measure the electron count.

Histidine

A .1M concentration solution at pH 7 with 2.7M KCl was examined by means of a step experiment. Electron counts of >200 were observed indicating that the carrier was not loaded as one might expect from its low binding constant. However, a most important observation is that the fractional conversion of complex measured by the current flowing was 45% at 0.5V without any addition of a catalyst. Electron transfer between the electrode and the cobalt complex is thus demonstrated to be very fast and that the amino acid structure may be important for fast kinetics.

Four new compounds have been screened including 34-2 Laura-methyl, 23-2 Laura-methyl and 22-2 Laura-methyl. These compounds complete the screening process for the 2-Laura-methyl series. Table 5 is a compilation of all the data collected on this series. In addition, a Tri(aminopropyl)amine. No significant current or oxygen output was observed with this compound.

Three of the originally planned four new EOC rigs were constructed and tested before the lab move. The rigs performed well except for the pumps which vapor locked due to the high gas output and the poor unloading efficiency. New pumps have been purchased which are more expensive but which will avoid this problem. The poor unloading efficiency has been the subject of discussion for the EOC Task Force group. Experiments have been carried out to compare pure oxygen unloading and air sweep unloading. These have demonstrated the inadequacy of our present unloader design for pure oxygen output and the task force will continue to experiment with this aspect.

The ligands used in the screening process summarized in Table 2 were prepared without extensive purification. The high electron count values particularly at low voltages indicate the presence of redox-active species which do not release oxygen. In some cases, this is due to the low binding energy such as for 34-2 Laura-methyl and was expected. However, the different experiments with 24-2 Laura-methyl have given electron count values as varied as 2.1 to 13.9. Indeed different experiments with the same batch of 24-2 Laura-methyl gave quite varied results.

Despite these contradictory observations, an important conclusion which can be drawn is that the mode of failure of the Laura-methyl series is quite different from the Suzy series. In all cases both the current and the oxygen output decreased with time so that although there may have been some rise in the electron count number of about 25-50% in no case was a catastrophic rise observed. In all cases for the Laura-methyl series the carrier simply faded away with both the current and the output decaying to unacceptable levels. Cleaning the cell or replacing felts or separators did not restore the performance. One observation of interest is that the longest lived of all the Laura-methyl compounds is the 23-2 L-me thus reinforcing the evidence already gained from the Suzy series that the 23 chain imparts extra stability.

Figure 13 compares the static stabilities of the carriers with the EOC stabilities. It is very striking that the static stabilities are much longer than the EOC stabilities for the Laura-methyl series while the opposite is true for the Suzy series. Our observations have been that the chemical degradation is predominant for the Suzy series and indeed the electrochemistry seems to prolong the carrier lifetime. The opposite is observed with the Laura-methyl carriers where the electrochemistry appears to shorten the lifetime.

These observations are compatible with the cyclic voltammetric data which clearly show that the oxidation of the oxygenated dimer complex gives a relatively stable superoxo species. Mechanistic schemes have been proposed whereby such species may lead to the formation of peroxide and indeed several of the Laura solutions turned red during the longevity tests:

$$\text{L-Co(II)-O}_2\text{-Co(II)-L} \Longleftrightarrow \text{L-Co(II)-O}_2\text{-Co(III)-L} + e^-$$

$$\Big\| \; H^+$$

$$\text{L-Co(III)} + {}^-\text{O}_2\text{H} \longleftarrow \text{L-Co(II)-O}_2\text{H}^+ + \text{Co(III)-L}$$

The source of the proton is unknown at present but it may come from the carrier molecule itself thus initiating degradation.

An alternative explanation for the behavior may lie in the purity of the carriers. Impurities may explain the irreproducible results and steps are being taken to investigate this possibility. However, initial results with purified 24-2-L-me seem to point to another explanation for the decreased lifetime.

Discussion

It should be noted that EOC experiments on ten different carriers were carried out during the course of the last quarter which is considerably higher productivity than was envisaged during the Liquid Air negotiations. The addition of the new rigs should allow us to more thoroughly evaluate the carriers and to look at more. Due to the rapidly increasing output of the synthesis group, this is very timely.

During this quarter we have achieved breakthroughs in a number of areas. First of all we have shown that carrier lifetimes of greater than one month are possible. We have shown that the very poor lifetime of 33SP is the exception rather than the rule and that carriers with lifetimes of greater length are very probable. WE have demonstrated that carriers with faster kinetics than 33SP are possible and that such fast kinetic carriers do not have to be more unstable than 33SP. Finally we have demonstrated that the electron transfer process between cobalt complexes and the electrode can be much faster than we have observed. The separate pieces of longer lifetime, faster oxygen release kinetics and very high fractional conversions have been demonstrated in different carriers. We also have shown that high current efficiencies can be achieved, a vital objective for us to claim any competitive advantage over 4 electron processes.

Figure 14 shows the status of our technology in terms of carrier longevity with respect to corporate goals.

Table 2

Lab book #	Ligand	Conc (mM/L)	Modulator	Conc	Flow	Amp	# e-/o2	L/ch o2	Power	% F.C.	Duration/Hyp
4WLC327A	33-2LMe	200			45	.51	4.30	1.00	147	3	10
4WLC*40	24-2LMe	50			60	.27	2.10	1.90	71	6	3
4WLC*4B	24-2LMe	50	DMMF	1	60	.45	2.20	3.70	75	10	10
4WLC329DB	24-2LMe	50	DMMF	1	60	.20	9.00	.14	179	0	72
4WLC329DB	24-2LMe	50	DMMF	1	60	.39	13.90	.42	457	16	192
4WLC329DD	24-2LMe	50	DMMF	1	60	.40	10.90	.56	350	17	144
4WLC329DD	24-2LMe	50	DMMF	1	60	.40	10.90	.56	359	17	120
4WLC329DD	24-2LMe	50	DMMF	1	60	.40	15.50	.40	508	17	160
4WLC329DD	24-2LMe	50	DMMF	1	60	.42	8.30	.77	270	17	96
4WLC331A	24-2LMe	50	DMMF	1	60	.23	3.90	1.10	104	5	2
4WLC331D	24-2LMe	50	DMM	1	60	.14	1.70	1.10	58	4	24
4WLC338A	24-2LMe	100			50	.06	1.90	.40	64	1	10
4WLC338DB	24-2LMe	100			50	.15	2.00	1.20	66	2	6
4WLC338D	24-2LMe	100	DMMF	1	50	.18	2.00	1.40	70	2	10
4WLC338C	24-2LMe	100	DMMF	1	50	.12	2.20	.80	72	1	40
4WLC339A	24-2LMe	50			50	.08	2.70	.45	90	2	20
4WLC339D	24-2LMe	50	DMMF	1	50	.24	3.10	1.20	104	6	5
4WLC339C	24-2LMe	50	DMMF	1	50	.24	2.20	1.60	73	6	24
4WLC344D	23-2LMe	100	DMMF	2	120	.36	9.80	.60	326	1	4
4WLC344C	23-2LMe	100	DMMF	2	120	.32	7.30	.68	249	2	10
4WLC347A	24-2LMe	100			50	.14	2.40	.09	80	2	10
4WLC347B	24-2LMe	100			100	.16	2.90	.84	95	1	4
4WLC347D	24-2LMe	100			25	.09	2.30	.60	76	2	4
4WLC347D	24-2LMe	100			50	.13	2.50	.80	81	2	4
4WLC347B	24-2LMe	100			75	.15	2.70	.05	87	1	4
4WLC347C	24-2LMe	100	DMMF	1	50	.13	3.10	.60	103	2	10
4WLC350A	24-2LMe	100			50	.11	3.60	.50	119	1	10
4WLC350B	24-2LMe	100			50	.25	4.10	.92	130	3	6
4WLC352A	23-2LMe	100			120	.12	3.00	.60	102	0	6
4WLC356A	22-2LMe	100			50	.05	6.00	.14	190	1	11
4WLC356A	22-2LMe	100	DMMF	2	50	.09	0.70	.10	300	1	20

Table 2 continued

Lab Book #	Ligand	Conc (uM/L)	Mediator	Conc	Flow	Amp	Energy	Pulse Width	Power	% E.E.	Duration/Dye
4WL C27B	33-2LMe	200			45	1.70	5.80	4.60	305	11	10
4WL C27D	33-2LMe	200			45	.10	6.50	.41	345	1	96
4WL C27B	33-2LMe	200			45	.24	5.70	.64	303	1	72
4WL C27B	33-2LMe	200			45	.44	4.00	1.40	210	1	48
4WL C27B	33-2LMe	200			45	1.10	4.90	3.50	260	4	24
4WL C29B	24-2LMe	50			60	.63	2.00	4.70	107	13	3
4WL C29D	24-2LMe	50	DMF	1	60	.82	2.20	5.60	117	17	10
4WL C31D	24-2LMe	50	DMF	1	60	.46	3.20	2.20	171	1	2
4WL C31D	24-2LMe	50	DMF	1	60	.10	2.90	.56	109	3	72
4WL C31D	24-2LMe	50	DMF	1	60	.11	3.20	.39	151	3	96
4WL C31D	24-2LMe	50	DMF	1	60	.19	3.70	.39	229	3	120
4WL C31B	24-2LMe	50	DMF	1	60	.19	2.30	1.10	100	5	48
4WL C33D	24-2LMe	100			50	.52	2.60	3.00	140	7	10
4WL C33BD	24-2LMe	100			50	.41	2.00	3.00	101	5	6
4WL C33D	24-2LMe	100	DMF	1	50	.30	2.40	2.00	146	4	10
4WL C33C	24-2LMe	100	DMF	1	50	.07	2.00	.35	101	1	96
4WL C33C	24-2LMe	100	DMF	1	50	.09	4.50	.30	216	1	120
4WL C33C	24-2LMe	100	DMF	1	50	.10	2.00	.76	100	1	72
4WL C35D	24-2LMe	50			50	.46	3.10	2.30	161	12	20
4WL C35D	24-2LMe	50	DMF	1	50	.40	2.70	2.70	139	10	5
4WL C44D	23-2LMe	100			120	1.00	4.10	3.50	216	5	10
4WL C44B	23-2LMe	100	DMF	2	120	1.30	5.40	3.70	281	3	4
4WL C44C	23-2LMe	100	DMF	2	120	1.30	4.00	5.00	200	7	10
4WL C44D	23-2LMe	100	DMF	2	120	.21	4.90	.66	294	2	168
4WL C44D	23-2LMe	100	DMF	2	120	.25	4.90	.80	290	2	144
4WL C44D	23-2LMe	100	DMF	2	120	.33	4.50	1.10	270	2	120
4WL C44D	23-2LMe	100	DMF	2	120	.42	3.80	1.70	221	3	96
4WL C44D	23-2LMe	100	DMF	2	120	.77	5.30	2.70	252	5	72
4WL C44D	23-2LMe	100	DMF	2	120	1.10	4.80	3.40	226	7	48
4WL C47D	24-2LMe	100			50	.52	2.50	3.00	131	6	10
4WL C47C	24-2LMe	100	DMF	1	50	.21	3.10	1.00	165	3	10
4WL C47D	24-2LMe	100	DMF	1	100	.52	2.20	3.60	102	3	4
4WL C47D	24-2LMe	100	DMF	1	25	.15	2.80	.84	103	4	4
4WL C47D	24-2LMe	100	DMF	1	50	.31	2.30	2.10	124	4	4
4WL C47D	24-2LMe	100	DMF	1	75	.42	2.20	2.90	132	4	4
4WL C49D	34-2LMe	100			50	.45	27.00	.25	1377	6	4
4WL C50D	24-2LMe	100			50	.50	4.00	1.90	209	6	18
4WL C50C	24-2LMe	100			50	.37	2.90	1.90	160	5	40
4WL C50C	24-2LMe	100			50	.52	2.40	3.40	130	7	24
4WL C52D	23-2LMe	100			120	1.90	5.00	5.60	203	6	6
4WL C54D	23-2LMe	100			120	.42	2.00	2.40	140	2	72
4WL C54D	23-2LMe	100			120	.42	3.00	2.00	150	2	48
4WL C54B	23-2LMe	100			120	.96	4.60	3.20	290	5	24

[illegible]	[illegible]	100			1.50	1.00	4.60	4.10	170	5	6
[illegible]	[illegible]	100			50	.97	3.00	1.00	224	5	10
[illegible]	[illegible]	100		2	50	.40	4.40	1.40	462	5	20
[illegible]	[illegible]	100	1000F	2	50	.12	5.60	.70	804	5	40
[illegible]	[illegible]	100	1000	2	50	.07	4.70	.90	540	4	20
[illegible]	[illegible]	100	1000F	2	50	.07	4.70	.90	540	4	20

Table 2 continued

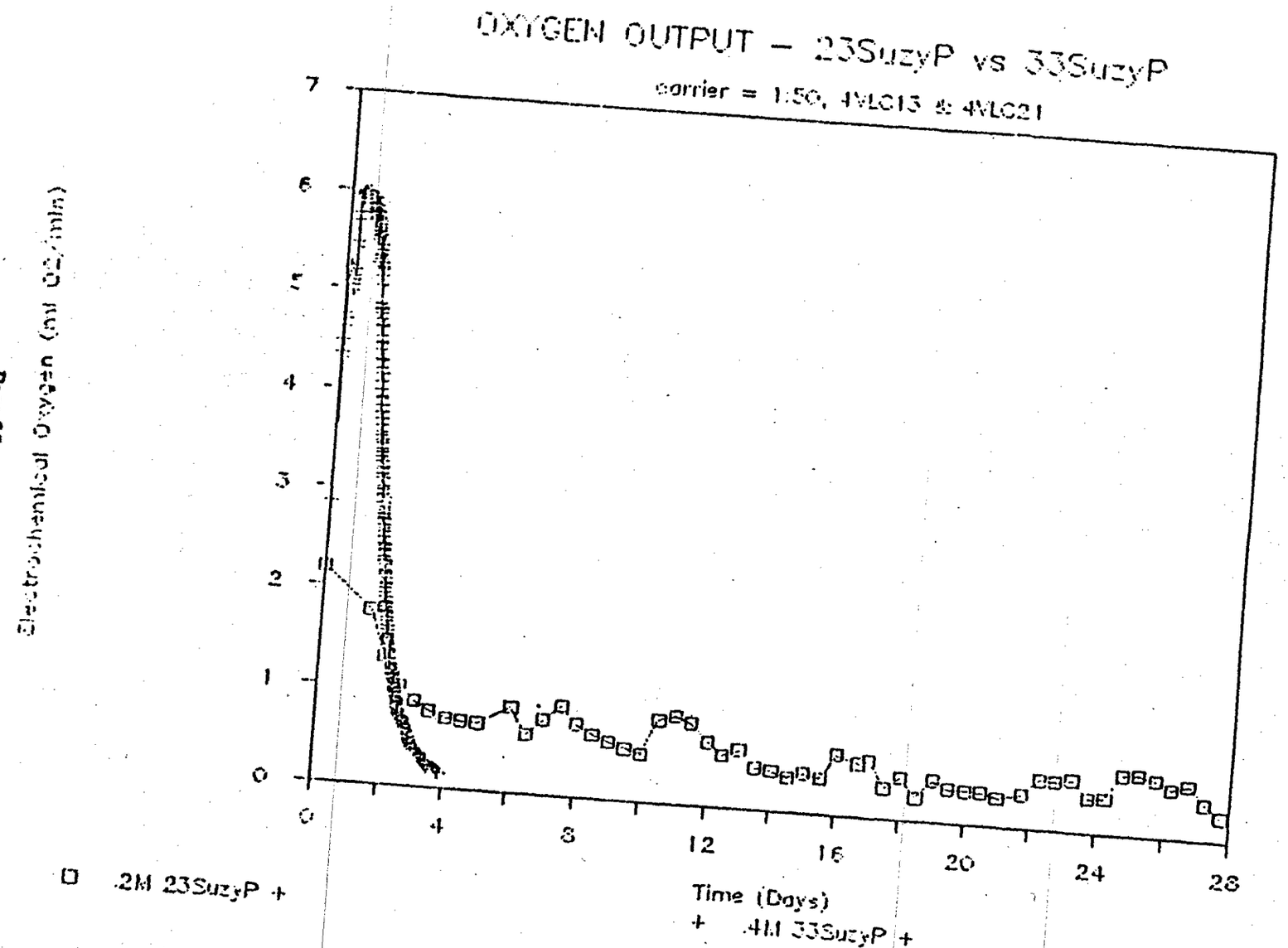
OXYGEN OUTPUT – 23SuzyP vs 33SuzyP
Carrier = 1:50, 4VLC13 & 4VLC21
Electrochemical Oxygen (nl O2/min)
0
1
2
3
4
6
7
0
4
8
12
16
20
24
28
Time (Days)
□ .2M 23SuzyP +
+ .4M 33SuzyP +

Figure 11

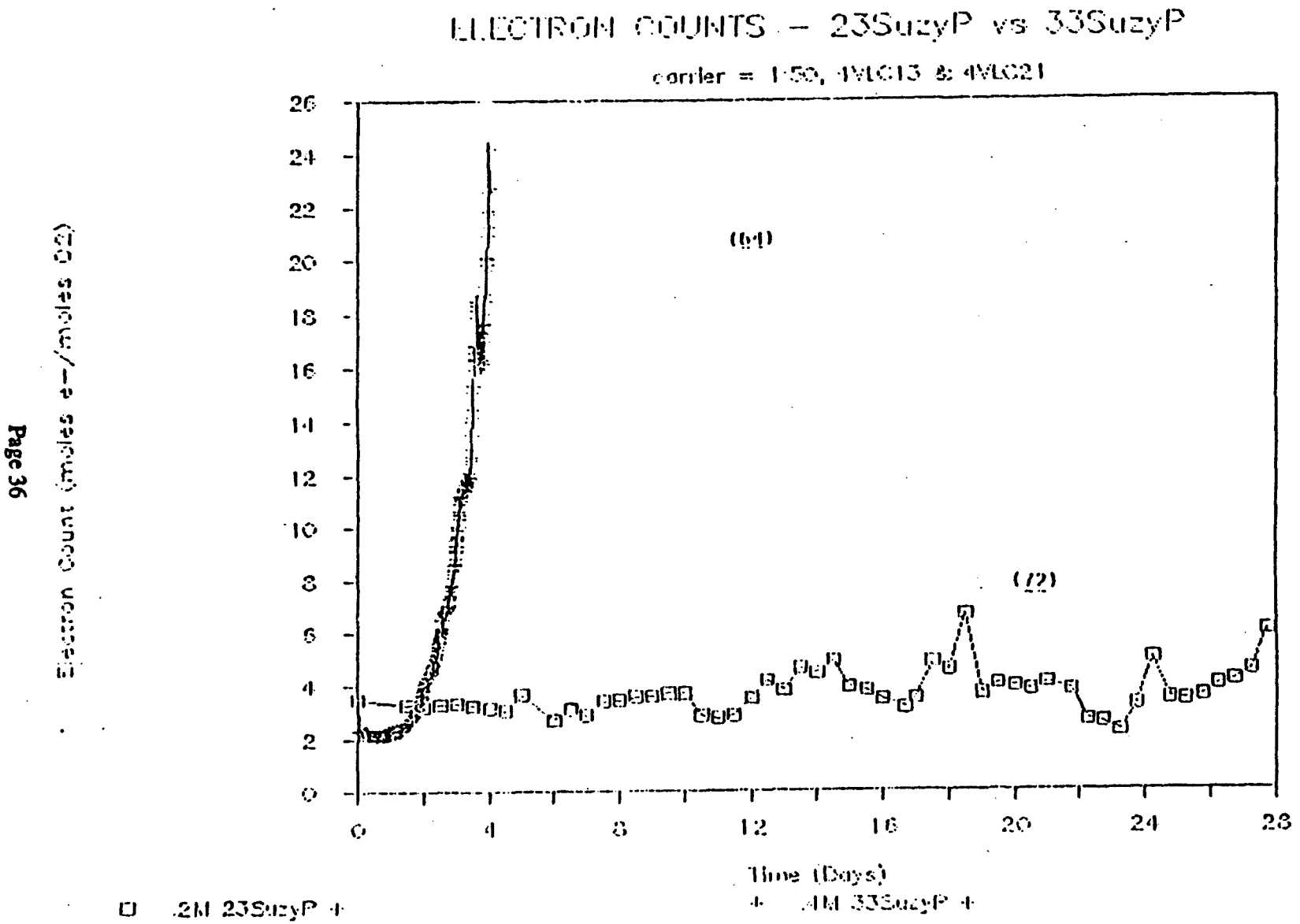
ELECTRON COUNTS – 23SuzyP vs 33SuzyP
corrler = 1-50, 4VLC13 & 4VLC21
Electron Count (moles e–/moles O2)
(64)
(12)
0
2
4
6
8
10
12
14
16
18
20
22
24
26
0
4
8
12
16
20
24
28
Time (Days)
.2M 23SuzyP
.4M 33SuzyP

Figure 12

Comparison of Spectroscopic and EOC Lifetimes

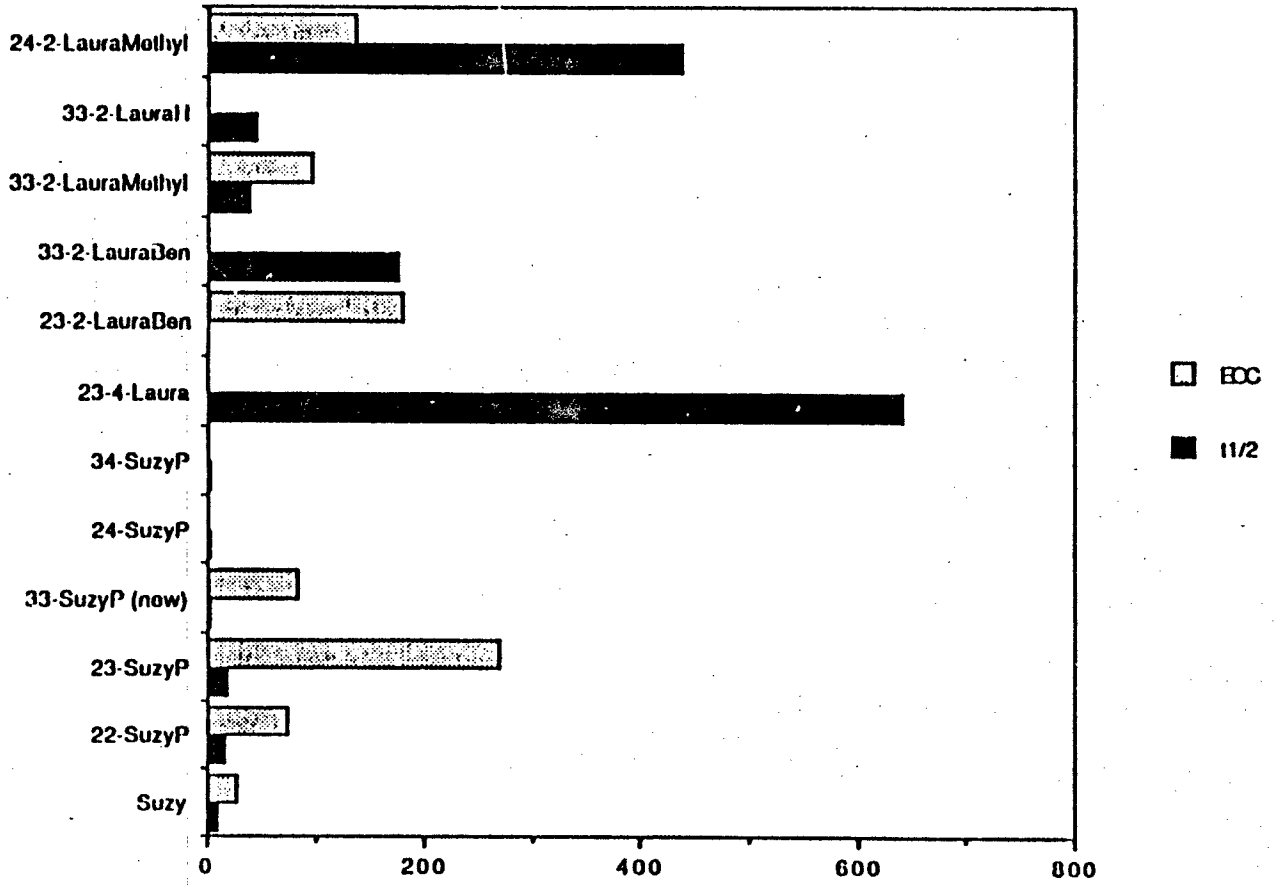

Figure 13

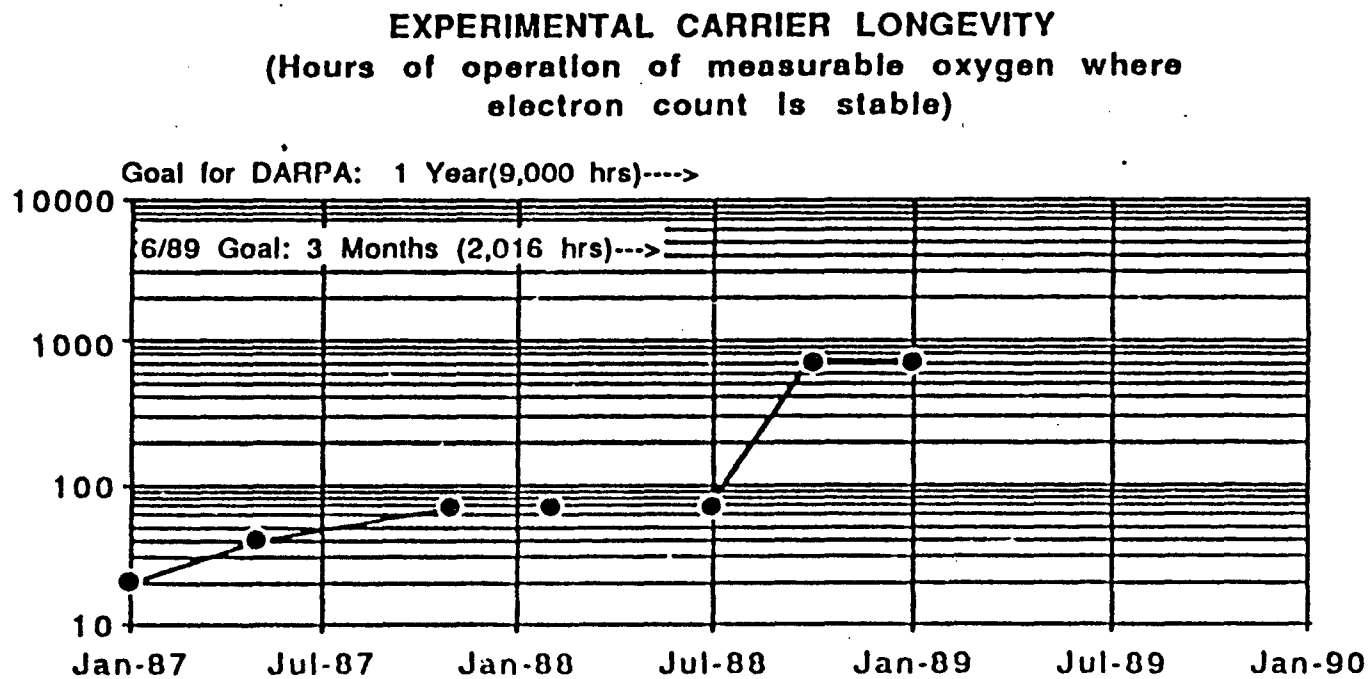
EXPERIMENTAL CARRIER LONGEVITY
(Hours of operation of measurable oxygen where electron count is stable)
Goal for DARPA: 1 Year(9,000 hrs)---->
6/89 Goal: 3 Months (2,016 hrs)--->
10000
1000
100
10
Jan-87
Jul-87
Jan-88
Jul-88
Jan-89
Jul-89
Jan-90

Figure 14

Objectives for Next Quarter

1) Complete construction of EOCs in new facility.
2) Continue to screen at least one new carrier per month.
3) Establish the effect of purity on the longevity and on the electron count levels.
4) Investigate a new mediator and a mediator-modified electrode.
5) Design very long term EOC in conjunction with L'Air Liquide.

3.B Kinetics

To make the Aquanautics system much better than competition, electrochemical kinetics should meet the design specs. The following section describes work carried out to meet the objectives.

Overview/Main Objectives

A. The objective for this section is to verify a combination of software and hardware suitable for rapid data acquisition on a single carbon fiber electrode.

Tafel plots obtained in 1988 deviate from an ideal "tafel" shape. In order to obtain kinetic parameters (rate constants and reaction alpha's), methods which use single carbon fiber electrodes are being explored. A program for evaluating kinetic parameters on single carbon fiber electrodes (SCFE's) was initiated during the first quarter. However, before using Professor Anderson's software for obtaining kinetic information on SCFE's, one needs to establish an appropriate time frame for data acquisition. Furthermore, one has to verify that there are no instrumental artifacts when obtaining data at high rates. This quarter LabTech Notebook was employed along with a re-configured tecmar data acquisition board. A National Electric VDG single carbon fiber electrode was used in a solution of Catalyst.

B. The objective for this section is to run a solution of 64/Catalyst in a planar gold cathode/gold anode EOC-size cell ($25cm^2$).

Summary, Results,and Discussion

A. Figure 15 shows a cyclic voltammogram of a National Electric VDG SCFE in a 4mM solution of Catalyst. One can observe that the returning reduction shows little current. Such behavior is expected when the electrode diameter is less than the diffusion layer: Catalyst ion created during the oxidation sweep can diffuse away from the electrode surface and be easily replaced by fresh Catalyst. Thus, this electrode conforms to the definition of a microelectrode and is suitable for the next series of experiments.

The latest tecmar labmaster data acquisition interface has a "DMA" feature suitable for the experiments outlined below. DMA means direct memory access: that is, an A to D conversion can be stored directly to memory without any further computer operations. Such a feature offers potential for rapid data acquisition.

Thus, the solution of 4 mM Catalyst is subjected to a positive potential step (0.6V vs. Ag/AgCl). Current generated at a SCFE is converted to a binary coded voltage via the interface and stored directly to memory. Two thousand data points at 25 microseconds per data point are acquired. Once finished with data conversion, the

digital data is further translated to an ASCI file (i.e., real voltages scaled to a current output). The integral of current over time results in the charge passed. Plots of charge versus the square root of time should be linear. The integrated Cottrell Equation predicts that such a plot should be linear with a slope proportional to species concentration, square root of the diffusion coefficient, number of electrons per mole of species, and the electrode surface area. For regions of non-linearity, one usually ascribes instrumental limitations (especially over short times) or convection currents stirring solution (long times).

The above experiment was also simultaneously recorded on a Iwatsu Digital Storage Oscilloscope at a similar 25 microseconds per data point.

Figures 16-18 show the resulting charge versus square root of time and residual versus square root of time plots. A residual is that value resulting from the actual charge and the charge predicted by a linear equation. The residual is a graphic technique for judging "goodness of fit" and a way to discern systematic error.

Several conclusions can be drawn from this experiment. First, the digital scope confirms the results obtained with the Tecmar-DMA and LabTech notebook software. Second, there is a systematic deviation from Cotrell linearity, especially at the very short (<1 millisecond) or long (>4.5 millisecond) time frame. However, a window between 1 and 4.5 milliseconds minimizes these deviations to an error of less than 5%.

While the above demonstrates the feasibility of fast data acquisition, several shortcomings prevent the use of the current set-up to evaluate kinetic parameters. LabTech Notebook's DMA feature does not allow voltage outputs (D to A signals). Thus, the successive voltage output steps needed for the Anderson kinetic routine would have to be programmed by hand. Hand initiation of the voltage step would affect the critical acquisition timing: spurious electrical signals from a mechanical thumbwheel on the potentiostat will erroneously trigger the acquisition.

However, if the newer tecmar-DMA interface boards are compatible with some of the older Fortran programs, then the custom data acquisition program provided by Professor Anderson could be used. The third quarter will evaluate this software on the newer tecmar boards.

REFERENCE: 8ED96 and references therein.

B. The planar pair of gold electrodes where evaluated in an EOC cell this quarter. A 0.4M solution of 64 was combined with 8mM Catalyst. The carrier was 100% reduced. A slow air sparge (around 4mL/min) was used in the unloader. Total gas flow is measured using the Omega Electronic Gas Flow Meter (10mL/min full scale range). A galvanic type oxygen probe monitored the exit gas. Figures 19 and 20 show the oxygen and current output for the high flow case (300mL/min). A lower flow was evaluated as well (70mL/min). Results are summarized below:

Flow LPM/M^2	Current Density mA/cm^2	Oxygen Output LPM/M^2	Cell Volt.
28	1.0	0.15	0.8
120	2.0	0.20	0.8

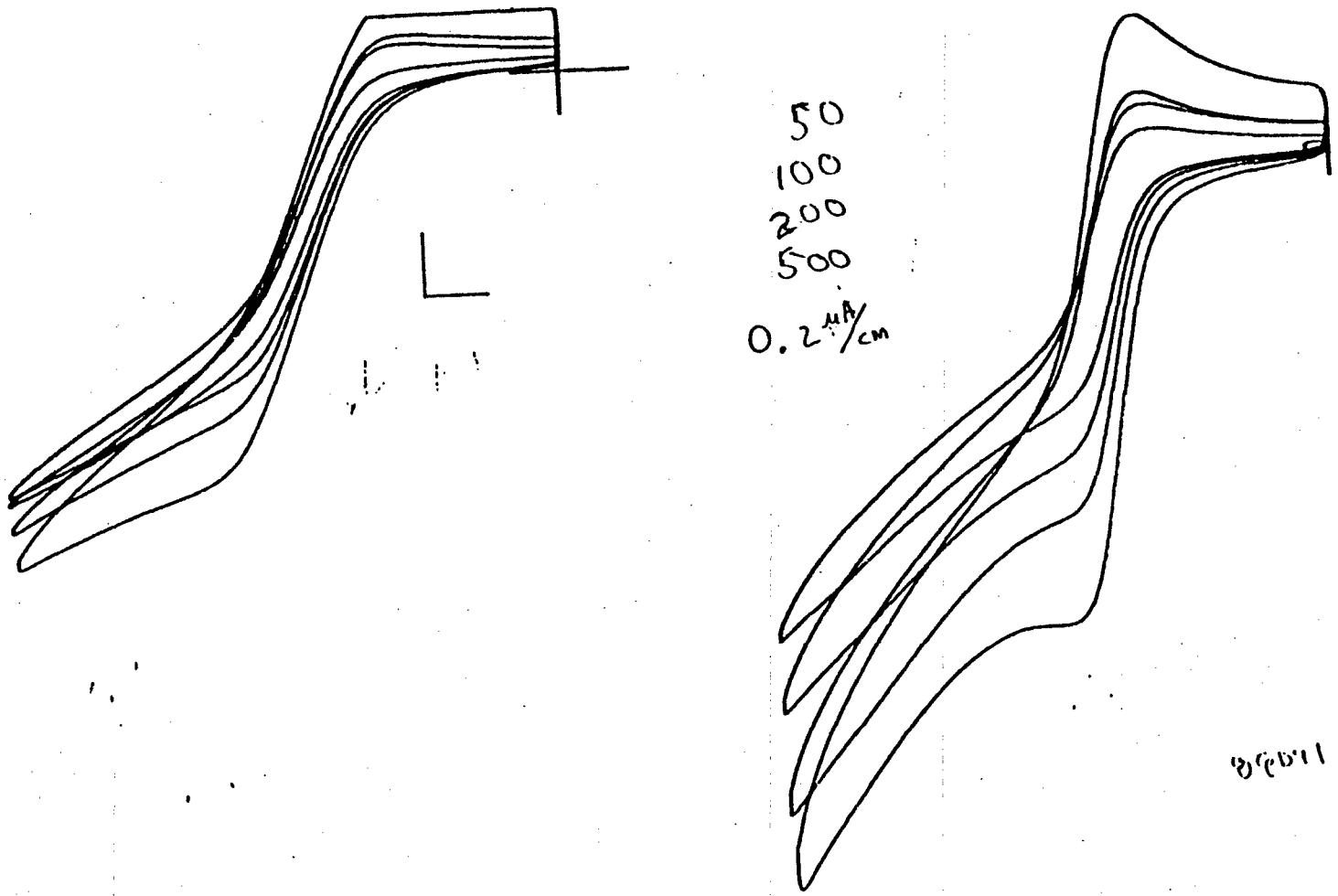

Figure 15

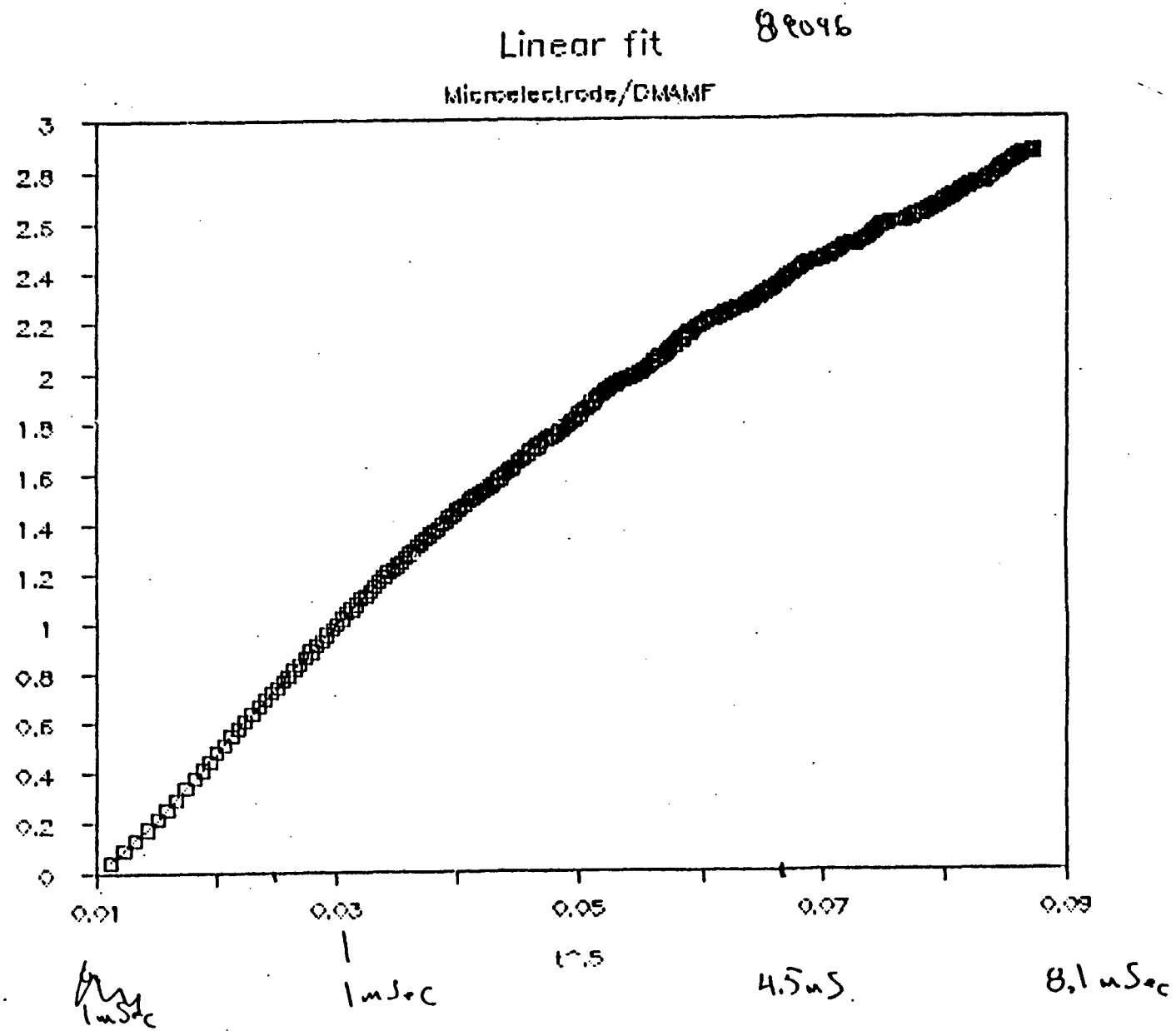
Linear fit
89096
Microelectrode/DMAMF
coul.
(Times 1E-10)
3
2.8
2.6
2.4
2.2
2
1.8
1.6
1.4
1.2
1
0.8
0.6
0.4
0.2
0
0.01
0.03
0.05
0.07
0.09
1mSec
1mSec
t^.5
4.5mS
8.1mSec

Figure 16

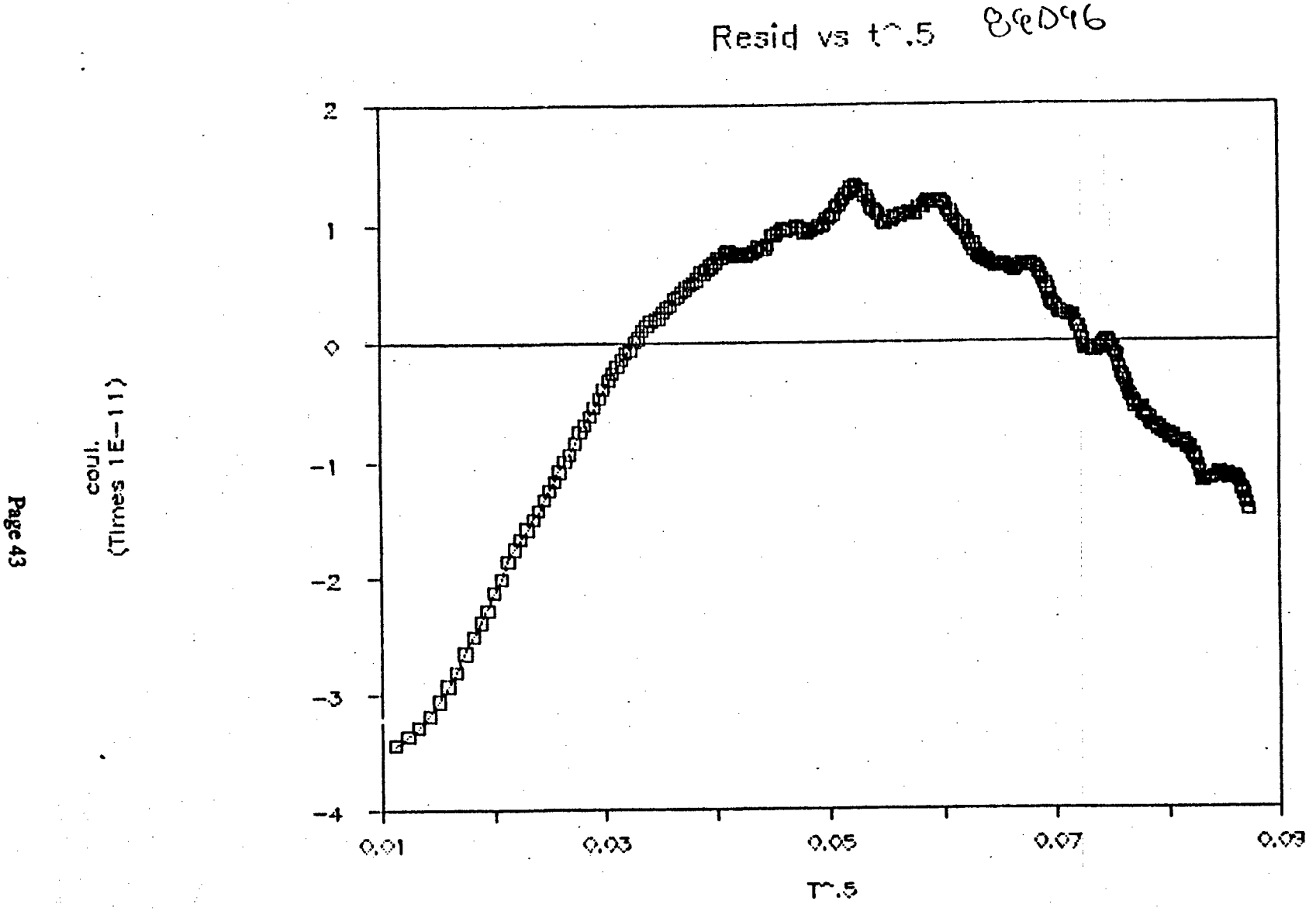
Resid vs t^.5
8eD96
coul.
(Times 1E-11)
2
1
0
-1
-2
-3
-4
0.01
0.03
0.05
0.07
0.09
T^.5

Figure 17

Resid vs. t 8E546

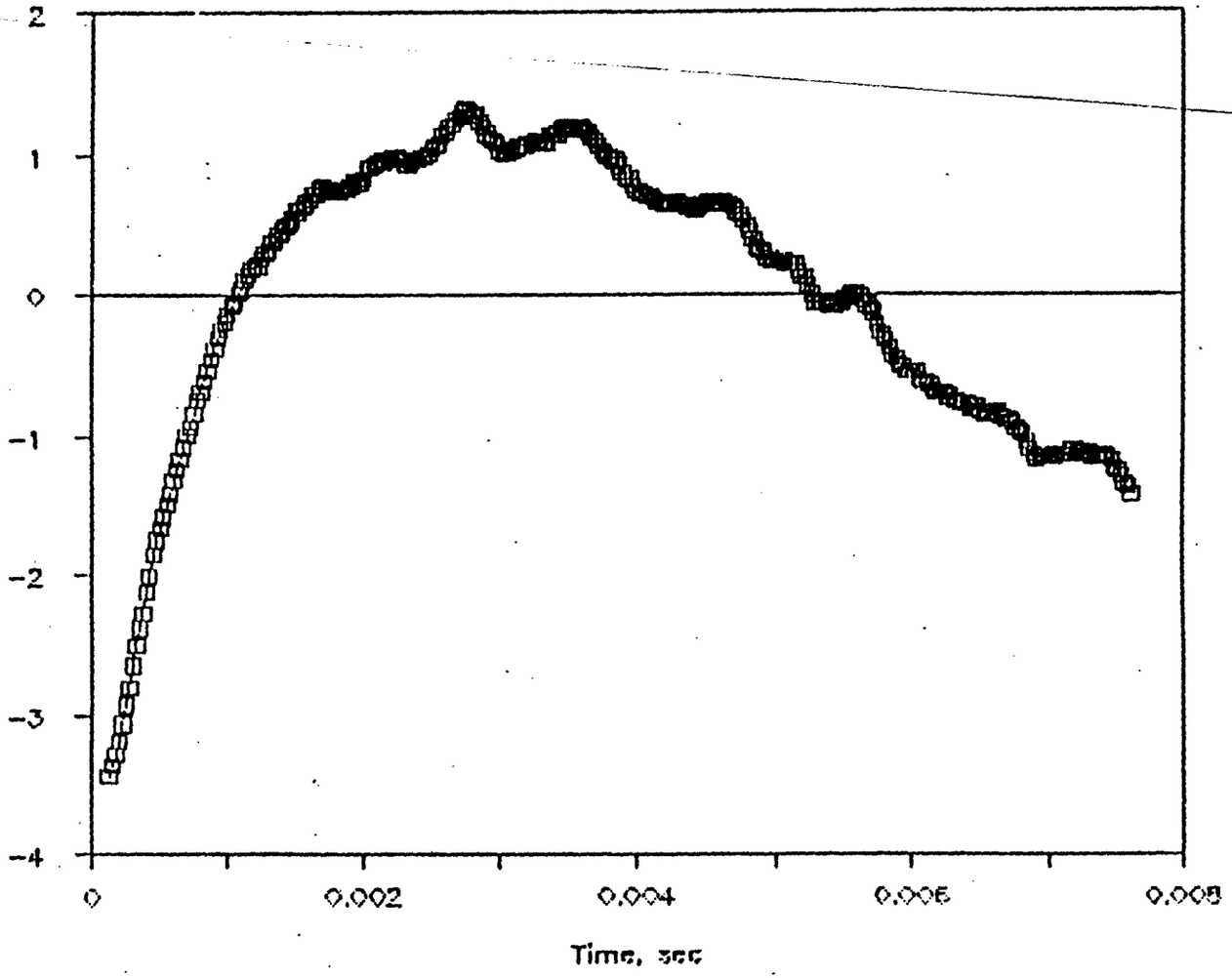

Figure 18

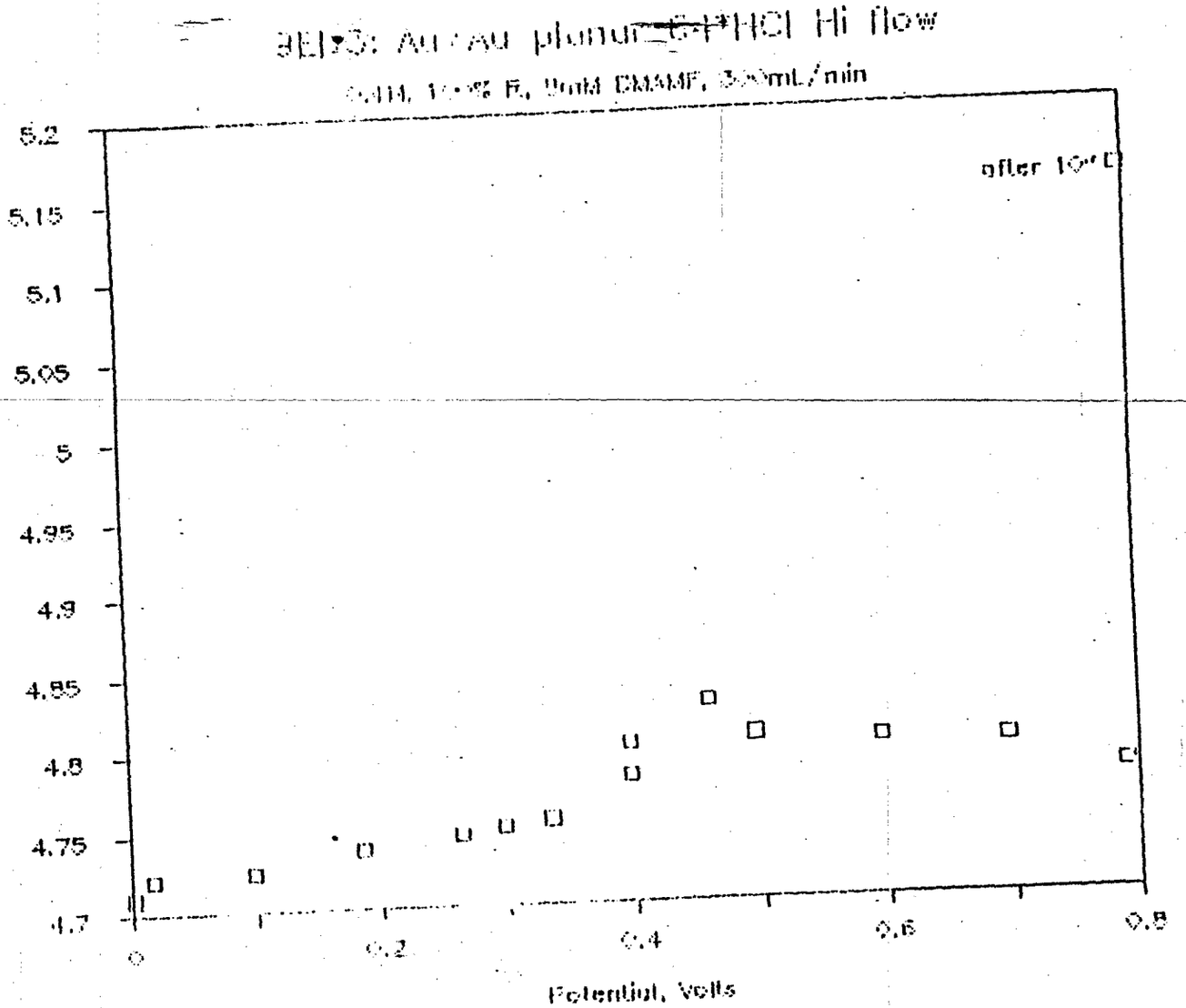

Figure 19

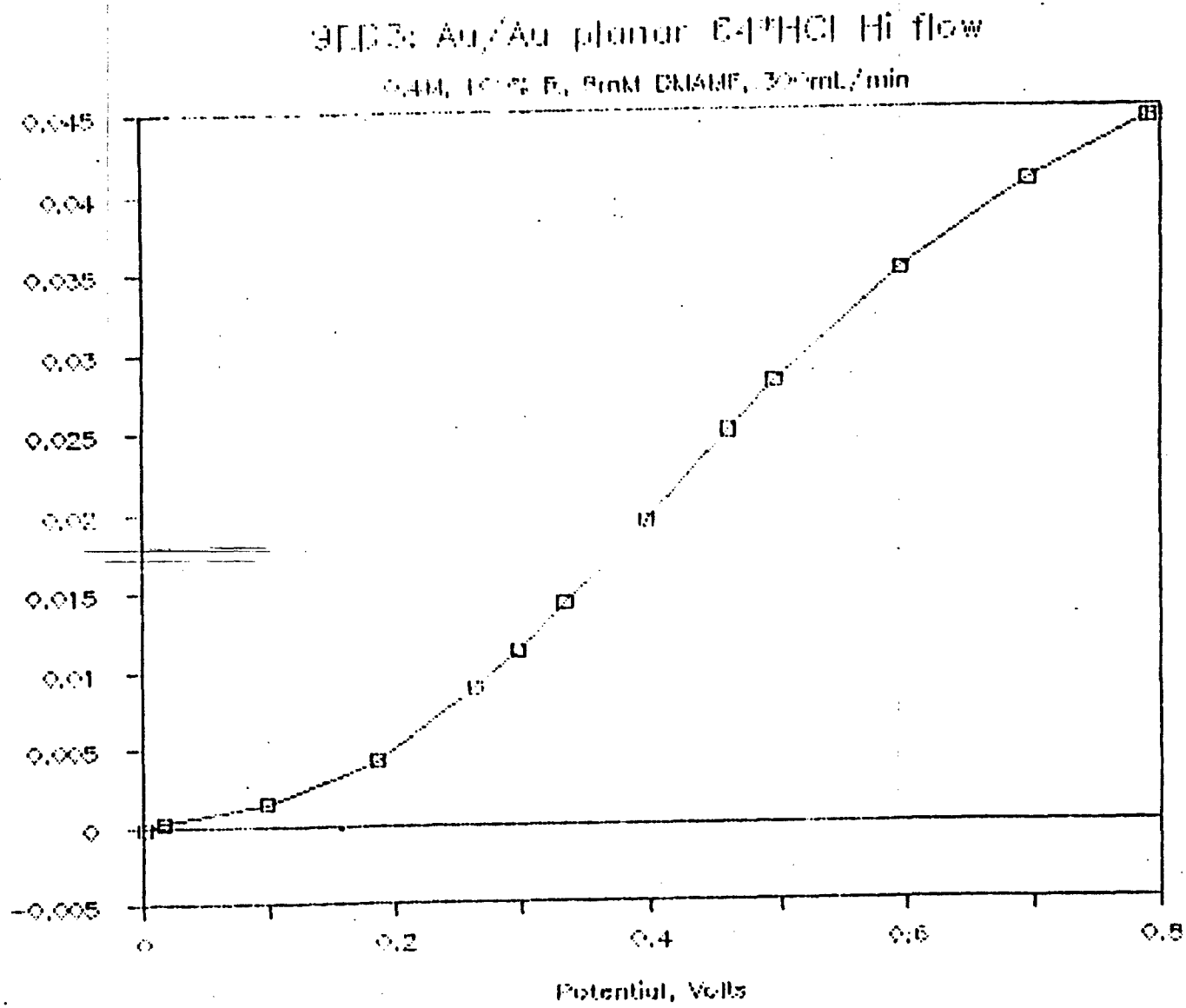
Current, amps
0.045
0.04
0.035
0.03
0.025
0.02
0.015
0.01
0.005
0
-0.005
0
0.2
0.4
0.6
0.8
Potential, Volts

Figure 20

Some attempts at depositing a layer of gold chloride on the cathode were made. Only a marginal increase in performance was noted.

These results tend to confirm J. Kerr's hypothesis that the rate limiting step for 64 is the dissociation step -not the electron transfer rate.

REFERENCES:9ED3 and references therein.

Appendix

Study of Hydrogen and Power Generating Characteristics of the Alwatt Underwater System

By

Alupower

(Report available on request)